



Cite this: *Soft Matter*, 2017, 13, 4931

## Thermodynamics of chemical Marangoni-driven engines

Rouslan Krechetnikov 

The goal of this paper is to perform a general thermodynamic study of Marangoni-driven engines in which chemical energy is directly transformed into mechanical motion. Given that this topic has not been discussed before, we will explore here the most basic and fundamental aspects of the phenomena at work, which leads to a number of interesting observations typical of controversies in classical thermodynamics. Starting with a discussion of a few key motivating examples of chemical Marangoni-driven phenomena – tears of wine, an oscillating pendant droplet, “beating” oil lens, and traveling waves in a circular container – and contrasting homogeneous *versus* inhomogeneous thermodynamic systems we naturally arrive at alternative ways of storing and generating energy with the help of inhomogeneities in the bulk and surface properties of the working media. Of particular interest here are systems with interfaces – hence, in this context we discuss the nature and efficiency of the corresponding thermodynamic cycles leading to work done as a result of a non-uniform distribution of surface tension, which is in turn induced by a non-uniform surface active substance (surfactant) distribution, for both soluble and insoluble surfactants. Based on the relevant physical parameters of the working medium we can also evaluate the isothermality, *i.e.* temperature variations, dissipative losses, energy output and efficiency, entropy generation, and the period of such cycles in real processes. The role of singularity formation at the interface for the existence of such thermodynamic cycles is unraveled as well. Finally the discussion is concluded with a few ideas for potential applications of Marangoni-driven engines.

Received 28th April 2017,  
Accepted 22nd June 2017

DOI: 10.1039/c7sm00840f

rsc.li/soft-matter-journal

## 1 Introduction

### 1.1 Motivation for non-Carnot cycle motors

The first law of thermodynamics is a statement of conservation of energy, *e.g.* for a closed system the change of the internal energy  $dU$  equals to the sum of the heat  $\delta Q$  received by the system and the work  $\delta W$  done on it:

$$dU = \delta Q + \delta W, \quad (1)$$

but this law does not say anything about the direction of these processes – this is taken care of by the second law of thermodynamics, namely that the total entropy  $S$  of an isolated system at a given temperature  $T$  cannot decrease

$$dS \geq \frac{\delta Q}{T}. \quad (2)$$

The basic laws (1) and (2) are at the foundation of our understanding of the efficiency of heat engines as homogeneous thermodynamic systems, *i.e.* systems with the thermodynamic properties (pressure, temperature, *etc.*) uniform throughout the

system extent. The Carnot cycle tells us that the maximum achievable coefficient of energy transduction should be  $(T_2 - T_1)/T_2$ , where  $T_1$  and  $T_2$  are the absolute temperatures of the cold and hot heat reservoirs, respectively. Therefore, a large coefficient of energy transduction requires a high heat of combustion or a large heat source.

On the other hand, all motor organs and organelles in living organisms work through the conversion of chemical energy directly into mechanical energy under almost isothermal conditions apparently with extraordinarily high efficiency and without producing harmful products.<sup>1</sup> This implies that biological motors operate through some mechanisms other than the Carnot cycle, and the induced motion is observed under non-equilibrium conditions, for example involving chemical inhomogeneity. Development of such a chemical engine, which works under (almost) isothermal conditions, is an important step in creating novel chemical motors or artificial actuators which are capable of self-movement, in understanding and creating biological functions,<sup>2</sup> as well as in providing new ideas on alternative autonomous energy sources for small-scale devices.<sup>3</sup> Inspiring examples include a crawling cell pushing its way through pores, while constantly changing its shape to adapt to a complex environment, and vesicles – closed surfaces of lipid bilayers – exhibiting an amazing variety of shapes,

Departments of Mathematical & Statistical Sciences and Mechanical Engineering,  
University of Alberta, Edmonton, AB T6G 2G1, Canada.  
E-mail: krechet@ualberta.ca; Fax: +1-780-492-6826; Tel: +1-780-492-1926

between which transformations can be induced by changing the osmotic conditions.<sup>4–6</sup> According to the modern view, the biological cell membrane is also a more or less fluid lipid bilayer in which proteins, including enzymatically active ones, are submerged and are often free to move.<sup>7–9</sup> The energy transformation in these biological motors is based on the dissipation of the chemical energy in adenosine triphosphate converted to adenosine diphosphate to drive molecular machinery; these highly efficient direct energy conversion processes take place within living organisms<sup>1</sup> such as amoeba pseudopod formation,<sup>10</sup> chloroplast movements,<sup>11</sup> swelling of mitochondria, and muscle contraction,<sup>12</sup> to name a few.

A fluid dynamics analogy where energy can be generated at the interface is a surfactant-laden system. It is known that below a saturation interfacial concentration for a given surfactant – near the critical micelle concentration (CMC)<sup>13,14</sup> – surface tension  $\sigma$  decreases with the bulk surfactant concentration  $C$ :  $d\sigma/dC < 0$ . Common surfactants, such as sodium dodecyl sulfate (SDS), can typically reduce the surface tension by approximately half of the clean interface value when the CMC is achieved<sup>15</sup> and, in the case of chemical reactions producing surfactant at the interface<sup>16</sup> – such as that between acid and alkali at the water–oil interface – may lead to ultra-low values of interfacial tension on the order of  $0.1 \text{ mN m}^{-1}$ , *i.e.* the surface tension changes two orders of magnitude. Such changes may occur both in time and space.

Dynamic, that is varying in time, surface tension (DST)<sup>†</sup> is an important driving property as it governs many important industrial and biological processes.<sup>17–20</sup> One biological process where the control of DST is essential is in the lung, where phospholipids are the main surface active ingredients: DST is necessary for effective functioning of the alveoli – understanding these processes led to the pulmonary surfactant replacement therapy,<sup>21</sup> where surfactant is responsible for lowering surface tension on expiration and preventing lung collapse, and to a treatment of dry-eye condition. In industry, DST is, of course, important in various emulsifiers and foaming agents. In fact, whenever surfactants are used, DST is a key effect: for example, in the photographic industry the formulation of thin gelatin films requires high flow velocities, and hence DST needs to be monitored during the fabrication process to prevent film deformation and irregularities. It is also of importance in agrochemicals where fast wettability of plant leaves is instrumental for easy spreading of pesticides. Not to mention that DST plays a crucial part in older technologies such as production of metal, paper and textiles as well.

From the point of view of variation in space, the surfactants' fundamental property of being an additional degree of control over fluid motion led to a growing number of engineering and bioengineering applications such as:

- non-mechanical means to pump and position fluids in microfluidic devices (*e.g.* flow cytometry, rapid DNA screening);<sup>22</sup>

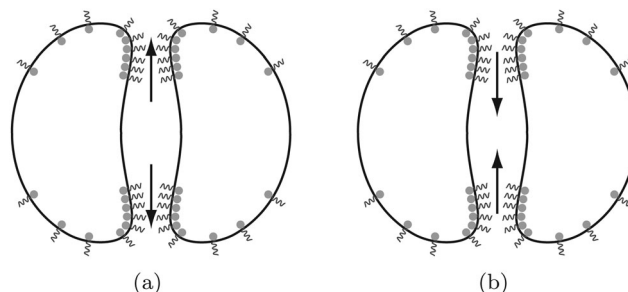


Fig. 1 When two water droplets containing a water soluble surfactant approach each other in an oil, an interfacial tension gradient is created by the bulk flow. (a) The oil trapped between the two droplets flows outwards sweeping the surfactant molecules toward the periphery of the separating film. Since the concentration of the surfactant molecules in the middle portions of the interfaces is lower in comparison with their concentration in the peripheral regions, an interfacial tension gradient is created. (b) This concentration gradient drives fluid – the so-called Marangoni flow – back to the center thus preventing the drops from merging and hence stabilizing the emulsion.

- enhanced oil recovery, in which surfactants have been used to effectively lower the interfacial tension between oil and water and enable mobilization of trapped oil through the reservoir;
- manufacturing integrated circuits and data storage for informational technologies, in which the coating processes are crucial.

At the fundamental level, numerous examples already exist in which Marangoni flows induced by spatial gradients in surfactant concentration at interfaces can be exploited in practice. These include the motion of droplets in the presence of externally imposed surfactant concentration gradients,<sup>23</sup> mixing of droplets having different values of surface tension,<sup>24</sup> spreading of surfactants,<sup>25</sup> and stabilization of emulsions by self-induced Marangoni effects which represent the basic example of the passive role surfactants may play, *cf.* Fig. 1, and of the nature of Marangoni-driven flow, for that matter. Also, surfactant-induced surface tension gradients proved to be responsible for the film thickening effect in coating on wires and plates.<sup>26–28</sup>

While Marangoni stresses can be created by temperature gradients,<sup>29</sup> imposing electric fields<sup>30–32</sup> and, as mentioned above, by passive addition of the surfactants,<sup>23–25</sup> all of these methods have shortcomings. For example, an imposed temperature gradient could be damaging to sensitive samples; moreover, such an approach for generating flow requires fabrication and control systems capable of establishing precise temperature gradients. Among the drawbacks of the electrochemical method to create Marangoni flows are (a) hostility of the solution needed for such applications, (b) reliance on imposed electric fields, which requires careful placement and control of electrodes to create and maintain the flow, and (c) necessity to remove surfactant from the surface either by diffusion into the bulk or oxidation using excess chemical constituents. Finally, surfactants simply added to a system generally play a passive role: established gradients are the result of other imposed conditions such as an external flow sweeping surfactants along the interface. Thus, on their own, surfactants usually do not tend to spontaneously create Marangoni-driven motion.

<sup>†</sup> A freshly formed interface of a surfactant solution has a surface tension  $\sigma$  very close to that of the solvent  $\sigma_0$ . Over a period of time,  $\sigma$  will decay to the equilibrium value,  $\sigma_{\text{eq}}$ , and this period of time can range from milliseconds to days depending on the surfactant type and concentration.

To overcome the shortcomings of the above methods used to induce Marangoni gradients, chemical reactions that produce surfactants at the interface can be exploited, which is the focus of the present work. The key distinction of this method from the aforementioned approaches is its autonomy, *i.e.* no dependence on external intrusion or electric/temperature fields.

## 1.2 Paper outline

In Section 2 we will begin by reviewing the key experimental observations which serve as a motivation for the present study of self-driven systems with direct conversion of chemical to mechanical energy. Here we focus on the general understanding of how Marangoni phenomena may mediate energy conversion and their subsequent usage. While the fundamental reason for self-sustained motion is a hydro-chemical Marangoni instability, which needs to be studied separately in each particular case,<sup>33,34</sup> instead we are going to focus on general thermodynamic aspects of the Marangoni phenomena. In Section 3 we review standard homogeneous thermodynamic systems and then extend the analysis to homogeneous chemical engines with some new results proved herein. This sets the stage for the analysis of inhomogeneous systems. With an idea to disentangle the complexity of self-driving Marangoni phenomena both at the energy and mechanistic levels, in Section 4 we first analyze the energy storage and the general dynamics of inhomogeneous systems in contrast to homogeneous ones. The goal here is also to understand the role of interfacial singularities in sustaining such motions. Then in Section 5 we address in detail the fundamental thermodynamic aspects – energy and entropy generation, thermal efficiency, and the extent of isothermality – of Marangoni-driven engines. Motivated by the practical questions on the feasible system geometries and physical conditions for the most efficient operation of self-sustained motions, in Section 6 we conclude the discussion with some ideas for potential engineering implementations.

## 2 Observations of Marangoni self-driven motions

Recent observations of fluid motions induced by the direct conversion of chemical-to-mechanical energy *via* chemical reactions at interfaces have renewed interest in this area and provided a hope for finding new ways to generate mechanical motion. The feasibility of engineering Marangoni-driven motors stems from a number of examples found both in nature and laboratory, some of which are familiar to a wide audience – water walkers<sup>35</sup> and camphor scrapings<sup>36,37</sup> – while others – such as the violent and erratic interfacial pulsations and localized eruptions of liquid–liquid interfaces<sup>38–41</sup> – have remained undeservedly forgotten. The classical example of self-induced fluid motions arising due to variations of interfacial tension is the self-propulsion of a small camphor scraping at an air/water interface, studied by Van der Mensbrughe<sup>36</sup> and Rayleigh<sup>37</sup> more than a century ago. Although a formal treatment of the solutal interfacial instability relevant to self-motion of camphor scrapings was given by Sterling and Scriven,<sup>34</sup> this

problem remains poorly understood from a quantitative standpoint in particular due to the lack of a complete thermodynamic picture. In recent decades, there has been a revival of interest in these types of problems,<sup>42–46</sup> which include self-induced motions of an aqueous droplet of the Belousov–Zhabotinsky reaction medium in an oil phase<sup>47</sup> and of an alcohol (pentanol) drop in an aqueous phase,<sup>48</sup> spontaneous oscillations of interfacial tension induced by a surfactant transfer through a liquid interface,<sup>49,50</sup> spatio-temporal periodic interfacial deformations due to chemo-Marangoni convection induced by *in situ* production of surfactant at the interface between hexane and alkaline solution,<sup>51</sup> various modes of motion (pulsation, rotation, *etc.*) of dissolving drops of dichloromethane,<sup>52,53</sup> and reactive droplets on a glass plate.<sup>54,55</sup> In particular, Dupeyrat and Nakache<sup>42</sup> found a quasi-periodic variation of the electrical potential and interfacial tension in an oil/water system, where a cationic surfactant was dissolved in the aqueous phase, and also reported macroscopic self-agitation at the oil/water interface. In this phenomenon, the chemical energy stored in the non-equilibrium of the solute concentrations between the oil and water phases is directly converted to macroscopic motion under, what was believed, isothermal conditions. To provide context for the present study, we will review a few examples of Marangoni effects inducing fluid motion in a self-sustained fashion as opposed to the passively acting surfactant-laden systems discussed in Section 1.

First, the phenomenon of “tears of wine”<sup>56–58</sup> – the formation and motion of drops of wine (and also other spirits) on the internal walls of a glass – has been observed since the early history of mankind, and its first description appears in the Bible. In lieu of the myths associated with the formation of the “tears”, a clear explanation can be given with surface tension gradients arising due to evaporation of alcohol from the mixture with water in the thin part of the meniscus where wine wets the glass surface – this in turn generates a gradient in surface tension and drives the fluid upward leading to formation of tears of wine, *cf.* Fig. 2.

The contact line (meniscus) plays a crucial role in another classical phenomenon reminiscent of the earlier mentioned self-motion of camphor scrapings – a self-propulsion of water

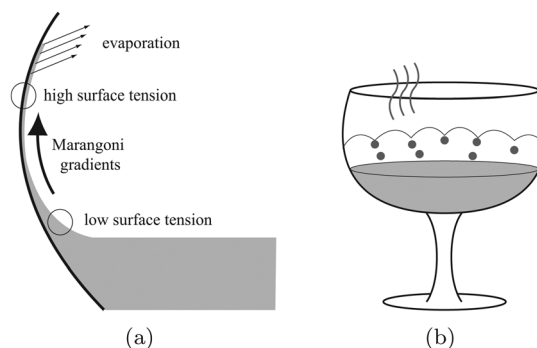
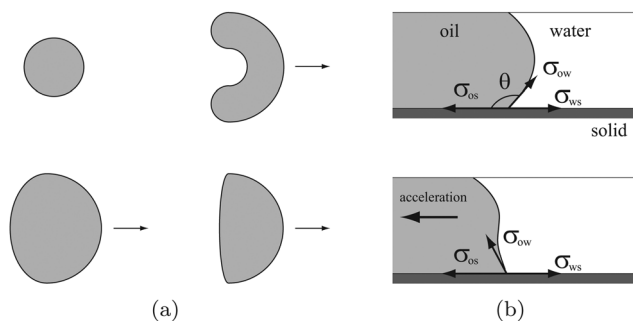


Fig. 2 Since water has a much higher surface tension than ethanol, a mixture of these liquids, such as wine, has a lower surface tension than that of pure water. (a) Mechanism: when alcohol evaporates from the thinner region of the meniscus, a surface tension gradient is generated, and the liquid climbs the glass wall spontaneously, forming a film and then, thanks to gravity, tears (b). The gradient is maintained by continuous evaporation of alcohol from the film, so that more liquid is dragged up.



**Fig. 3** (a) Amoeba-like motions in an oil/water system (top view): the oil phase is a nitrobenzene solution of iodine and potassium iodide and the aqueous phase contains a cationic surfactant. (b) Mechanism: inversion of the contact angle  $\theta$  induced by a sudden increase in tension  $\sigma_{ow}$  between the oil and water phases is essential for producing marked acceleration in the self-motion of the oil droplet based on Young's equation  $\sigma_{ws} = \sigma_{os} + \sigma_{ow} \cos \theta$ .

drops containing cationic surfactants after they are placed in an oil phase (nitrobenzene solution of iodine and potassium iodide),<sup>44</sup> cf. Fig. 3. The self-motion was observed to continue for 30–60 min until all the chemicals (“nutrients”) are “digested”.

Similar to the motion of camphor scrapings but without propulsion, quasi-periodic radial pulsations of an oil lens containing a water-insoluble surfactant (Tergitol) atop a water layer were observed,<sup>59,60</sup> cf. Fig. 4. The phenomenon was attributed<sup>61</sup> to a combination of partial emulsification at the edge of the lens and transport/evaporation of surfactant at the liquid–liquid interface resulting in a time-dependent spreading and can be related to other observations of spreading/contracting lens<sup>62</sup> involving chemical

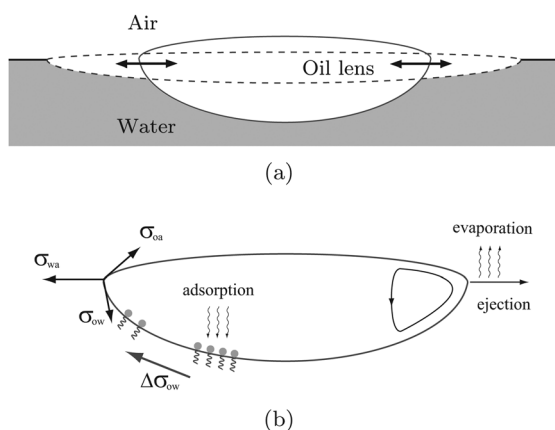


**Fig. 4** (a) Oscillating liquid lens (side view). (b) Mechanism: (i) adsorption of the oil-soluble surfactant onto the lens-water interface reduces  $\sigma_{ow}$  and evaporation of surfactant from the water surface increases  $\sigma_{wa}$ , causing the lens to expand; (ii) differential adsorption generates a radial surface tension gradient  $\Delta\sigma_{ow}$  that drives a circulation in the outer annulus of the lens. The lower surface of the lens becomes unstable to a series of radially propagating waves that sweep surfactant onto the water surface, reducing  $\sigma_{wa}$  and causing the lens to contract due to Young's equation: e.g. the net force balance at the triple point projected on the horizontal axis gives  $\sigma_{wa} + \sigma_{oa} \cos \alpha + \sigma_{wo} \cos \beta = 0$ , where  $\alpha$  is the contact angle between air and oil and  $\beta$  between water and oil. Evaporation reduces the Tergitol concentration on the water surface thereby reinitializing the system.

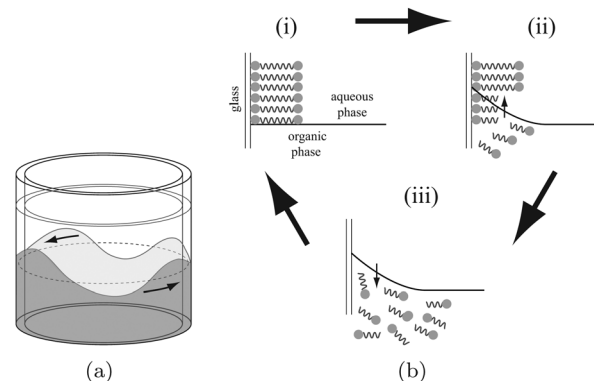


**Fig. 5** (a) Rotating chemical waves in an annular container (side view). (b) Mechanism: (i) adsorption of TSAC bilayer on the glass surface; (ii) upward motion of contact line with desorption of outer leaflet, which leads to the change in contact angle; (iii) desorption of the remaining TSAC monolayer due to chemical reaction with the oil soluble anion, which results in downward motion of contact line back to its initial position.

reactions. Only a limited range of surfactant concentrations (4–25%) was explored because of the sporadic nature of oscillations outside of this range.

In a very different geometry, Marangoni-induced wave patterns and surface oscillations (both regular and aperiodic) were observed<sup>47,63</sup> in annular containers, cf. Fig. 5. Two immiscible liquids of different density containing reagents – water with the trimethyl stearyl ammonium chloride surfactant (TSAC) and nitrobenzene with iodine – were initially stratified and quiescent prior to the initiation of spontaneous sustained waves lasting on the order of 10 minutes. As noted first by Kai *et al.*<sup>63</sup> and later by other authors,<sup>64</sup> the change in contact angle plays the crucial role in wave generation, cf. Fig. 5.

As a stand-alone example, several studies have revealed unusual phenomena associated with the production of surfactant at immiscible liquid–liquid (e.g. oil–water) interfaces. These include, cf. Fig. 6, the discovered<sup>65,66</sup> self-oscillation of a pendant drop and chemical-reaction-driven tip-streaming, in which micron sized droplets are produced from the tip of a millimeter scale drop when it assumes a conical shape. Self-sustained oscillations of the pendant drop were observed to accompany this behavior lasting on the order of 20 minutes or longer. The surfactant, which is a driving agent here, was produced at the interface *via* chemical reaction between reagents – alkali (NaOH) in the water and linoleic acid in the oil phases. There are other phenomena reminiscent of this self-induced tip-streaming including droplet emission in dissolving drops of dichloromethane,<sup>52</sup> ejection of surfactant-coated oil droplets from surfactant-laden sessile oil lens placed on a water surface,<sup>61</sup> and fission of an alcohol (pentanol) drop in an aqueous phase.<sup>48</sup>

All the aforementioned studies were primarily observational as the authors did not attempt to control the spatial production of surfactants or variations in surface tension, unlike in the case of the externally imposed electric, temperature, and concentration fields. Nevertheless, the above described experiments on the spontaneous and sustained motion of fluid interfaces resulting from chemical reactions are the most promising starting points to further the study of direct conversion of chemical energy into mechanical

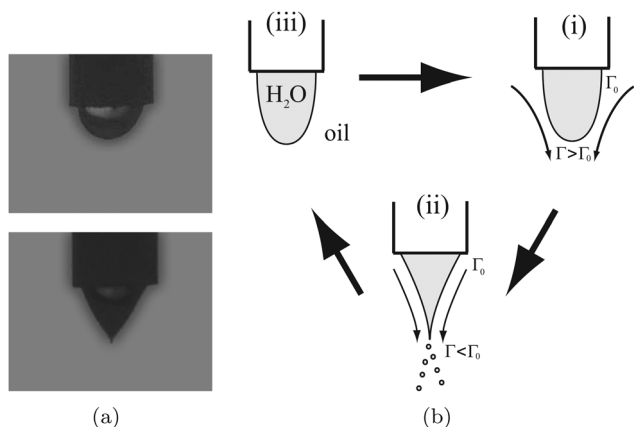


**Fig. 6** (a) A pendant drop driven by Marangoni effects at the water–oil interface (side view). (b) Mechanism: when interfacial surfactant concentration  $\Gamma$  reaches a critical value  $\Gamma_c$ , its magnitude is suddenly reduced by  $\Delta\Gamma$  in the process of tip-streaming. Once triggered, the following sequence of repeating events takes place: (i) sweeping surfactant towards the tip of a pendant drop, which facilitates the tearing up of the interface; (ii) tip-streaming, which removes surfactant from the drop and thus increases interfacial tension; (iii) drop relaxation back to a round shape due to the increased interfacial tension at its tip with the newly created surfactant concentration gradient between the base and the tip of the drop driving Marangoni flow.

motion at the fundamental level. The common features shared by the systems considered in Fig. 2–6 are: operation under almost isothermal conditions (which has not been quantified experimentally, however), the inhomogeneous character (*i.e.* non-uniform distribution of surfactant concentration and hence surface tension), and interfacial singularities, obvious and less obvious ones: (a) cone-tip/cusp singularity of pendant drop in Fig. 6 and spontaneous emulsification in Fig. 4, and (b) contact line singularity in Fig. 2, 3 and 5. The most apparent singularity is tip-streaming in Fig. 6, which exhibits itself as a cone-tip or cusp from a macroscopic perspective, though the contact line singularity is known to have a multiscale nature as well. In both cases the singularities are responsible for the removal/transport of surfactant from the interface. In the oscillating pendant drop case the surfactant is removed by tip-streaming and in all other cases either evaporation or sorption occurs near the contact line, which leads to the change of the contact angle and thus propulsion, *cf.* Fig. 3–5, or transport of the bulk fluid dragged by Marangoni stresses – the latter effect is present in all systems, but plays the key role in the phenomena shown in Fig. 2, 5 and 6. All these observations motivate the corresponding questions on their fundamental nature and role in sustaining macroscopic motion. Finally, as will be argued in Section 6, symmetries – such as in the oscillating lens – and asymmetries – such as in the pendant drop – present in all these examples enable their use, if properly harnessed, as engines in a number of applications.

### 3 Homogeneous systems

To set the stage, let us first consider homogeneous systems, *i.e.* systems with uniform thermodynamic properties (temperature  $T$ , pressure  $p$ , *etc.*). First, we will briefly review the classical

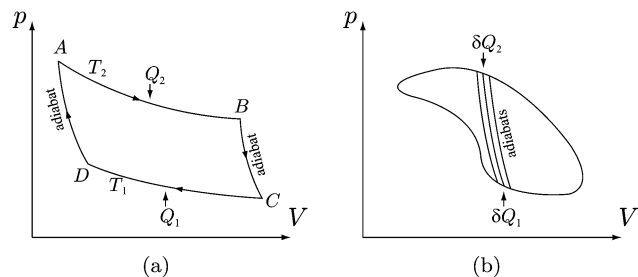


**Fig. 7** Thermal Carnot cycles for standard (a) and general (b) homogeneous systems.

Carnot cycle (Section 3.1) and then translate the analysis onto homogeneous chemical systems (Section 3.2).

#### 3.1 Heat engines

As we know from classical thermodynamics, the basic idea of a heat engine is during one cycle to receive the heat  $Q_2$  from the hot reservoir, to give the heat  $Q_1$  to the cold reservoir, and to perform the work  $-W$ , where negative sign accounts for the convention in the first law (1) that  $W$  represents the work done on the system.

In cyclic processes, *cf.* Fig. 7, the internal energy of the system does not change,  $\Delta U = \oint dU = 0$ . Hence, integrating the first law (1) one obtains  $0 = \oint \delta Q + \delta W = Q_2 - Q_1 + W$ , so that the work done by the system is  $-W = Q_2 - Q_1$ , *i.e.*  $Q_1$  is the heat wasted, and hence the engine efficiency is

$$\eta = \frac{-W}{Q_2} = 1 - \frac{Q_1}{Q_2} \leq 1. \quad (3)$$

The total entropy change must be zero due to reversibility of the Carnot cycle: $\ddagger$

$$\frac{Q_1}{T_1} - \frac{Q_2}{T_2} = 0. \quad (4)$$

An infinite number of such infinitesimal Carnot cycles can be used to represent a general cyclic process with  $T$  changing arbitrarily, *cf.* Fig. 7b – in this case adiabats cancel each other, which brings us to the Carnot theorem.

**Theorem 1 - Carnot's theorem.** The efficiency of any reversible heat engine operating between heat reservoirs with temperatures  $T_1$  and  $T_2$  is equal to the efficiency of Carnot engine:

$$\eta = 1 - \frac{T_1}{T_2}. \quad (5)$$

Under more realistic assumptions about heat transfer than typically made in reversible thermodynamics, endoreversible thermodynamics<sup>67</sup> shows that one has to give up the condition of an infinitesimal temperature gradient required to achieve the Carnot efficiency with the resulting infinitesimally small power. Instead, the engine operates at the temperatures  $T_1'$  and  $T_2'$  while in contact with cold  $T_1$  and hot  $T_2$  reservoirs, respectively. Thus, realizing that any transfer of heat between two bodies at differing temperatures is irreversible<sup>67</sup> and that non-

$\ddagger$  Because  $T$  and  $S$  are state variables, they are the same at the end of a cycle, but  $\delta Q$  can be non-zero because  $TdS$  is not a full differential.

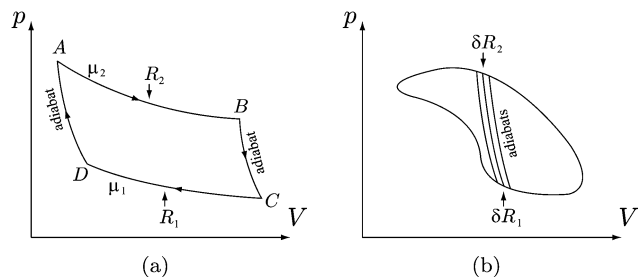


Fig. 8 Chemical Carnot cycles for standard (a) and general (b) homogeneous systems.

infinitesimal power is sought, by optimizing power over the actual engine temperatures  $T_1'$  and  $T_2'$  one gets instead the efficiency:

$$\eta_{\text{endo}} \leq 1 - \sqrt{T_1/T_2}, \quad (6)$$

which is obviously lower than the Carnot efficiency.

### 3.2 Chemical engines

One can translate the above analysis to homogeneous chemical engines with the first law (1) now written as

$$dU = \delta Q + \delta W + \mu dN, \quad (7)$$

where the last term stands for an increase of internal energy due to adding  $dN$  particles of chemical potential  $\mu$  (for simplicity a single-component system is considered).

First, taking for clarity of exposition  $T = \text{const}$  so that  $\delta Q$  is a perfect differential  $\delta Q = TdS = d(TS)$  and hence  $\delta Q = 0$  over the cycle, and recalling that for reversible processes  $\delta Q = TdS$  and  $\delta W = -pdV$  we can see the direct analogy between the chemical potential  $\mu$  in chemical engines and the temperature  $T$  in heat engines, and the same for the number of particles  $N$  versus entropy  $S$ . This consideration brings us to the cycle in Fig. 8, in which chemical energy  $\delta R \neq 0$  is supplied when  $\mu = \text{const}$  and there is no chemical energy exchange,  $\delta R = 0$ , on ‘adiabats’. Another way to think about the cycle in Fig. 8 is that, first,  $\mu_2$  is supplied and then spontaneously (irreversibly) converted into  $\mu_1$  and removed from the system in the same way as heat is removed from the heat engine: this is, of course, not surprising as both heat and chemicals are transported by the same mechanisms, e.g. diffusion – in the former case it is called Fourier’s law and in the latter Fick’s law. Such a change in the chemical potential can be achieved in a number of ways. Proceeding as in Section 3.1, we find that the work done by the system is  $-W = R_2 - R_1$ , so that the efficiency is

$$\eta = \frac{-W}{R_2} = 1 - \frac{R_1}{R_2} \leq 1. \quad (8)$$

§ We keep the term “adiabatic” since its meaning, based on Greek origin, is “impassable”, i.e. in this case impassable to chemical energy flow.

¶ For example, higher concentration of molecules corresponds to their higher chemical potential, which is why they migrate to the area of lower concentration, where their chemical potential lowers; e.g. the chemical potential for a non-ionic surfactant as a function of bulk surfactant concentration  $C$  is  $\mu = \mu^{(0)} + k_B T \ln C$ .

If we treat the “high” and “low” chemical energy reservoirs as a huge “adiabatic” body, then the increase in the total number of particles is

$$\frac{R_1}{\mu_1} - \frac{R_2}{\mu_2}, \quad (9)$$

but it must be zero for a cyclic process, which leads us to the analog of the Carnot theorem for a general chemical cycle in Fig. 8b.

**Theorem 2 - chemical Carnot’s theorem.** The efficiency of any reversible chemical engine operating between chemical reservoirs with potentials  $\mu_1$  and  $\mu_2$  is equal to the efficiency of chemical Carnot engine:

$$\eta = 1 - \frac{\mu_1}{\mu_2}. \quad (10)$$

Applying the same reasoning as for thermal endoreversible engines,<sup>67</sup> i.e. assuming that the real chemical engine has the chemical potentials  $\mu_1 < \mu_1'$  and  $\mu_2' < \mu_2$ , which according to Fick’s law of diffusion guarantee that the chemical transport is not infinitesimally slow, and then optimizing the power output over possible values of  $\mu_1'$  and  $\mu_2'$ , one arrives at the efficiency  $\eta_{\text{endo}} \leq 1 - \sqrt{\mu_1/\mu_2}$  similar to the efficiency of endoreversible heat engines (6).

If  $T \neq 0$  and not constant, then there could be heat generated during the chemical cycle since  $TdS$  is no longer a full differential (so that its integration over the cycle gives a non-zero area). Note that instead of  $(p, V)$  variables in the expansion work, one can apply the same analysis for the work done by surface tension, i.e.  $\delta W = \sigma dA$  in the  $(\sigma, A)$  plane with the obvious modification of (7). Thus the two basic cases correspond to the work done by the bulk and by the interface, respectively:

- Bulk only: from  $0 = \oint (\delta W + \delta Q + \delta R)$  we find  $-W = Q_2 - Q_1 + R_2 - R_1$ , which gives the efficiency

$$\eta = \frac{-W}{R_2 + Q_2} = 1 - \frac{R_1 + Q_1}{R_2 + Q_2}, \quad (11)$$

i.e. the input now is a combination of chemical and heat energies  $R_2 + Q_2$ , where  $Q_2$  is the heat generated by a chemical reaction and thus contributes to the work done by the bulk  $\delta W = -pdV$ .

- Interface only: the heat  $Q_2$  generated by a chemical reaction does not contribute much to the (non-expansion) work done by surface tension  $\delta W = \sigma dA$  and hence can be neglected as a useful input

$$\eta = \frac{-W}{R_2} = 1 - \frac{R_1}{R_2} - \frac{Q_2 - Q_1}{R_2}, \quad (12)$$

in which case  $Q_2$  contributes to losses. Hence, the advantage of isothermal reactions is that  $TdS$  becomes a full differential and, since entropy  $S$  is a state variable,  $\oint TdS = 0$ , so that  $(Q_2 - Q_1)/R_2$  vanishes in (12) and the expression reduces to (8).

If the work is done by both bulk and interface, then for  $T = \text{const}$  (and hence  $\delta Q = 0$  over the cycle) the most useful work (in terms of displacement) is done by the surface tension  $\sigma dA$ , so the bulk is passive here as  $dV \approx 0$ . To prove the latter point, let us consider a liquid drop as a working body and determine the interfacial displacement in the case when all the work done

by surface tension forces goes to the volume change  $\Delta V$  of the drop of volume  $V_0$ :

$$\frac{\Delta V}{V_0} \approx -\frac{\Delta p}{K}, \quad (13)$$

where the bulk modulus of water at moderate pressure is  $K = 2.2 \times 10^9$  Pa and from the capillary forces balance  $\Delta p \approx 2\Delta\sigma/R_0$ , which gives for  $\Delta\sigma = 0.1$  N m<sup>-1</sup>:

$$\Delta R \approx -\frac{2\Delta\sigma}{3K} = 10^{-10} \text{ m} = 1 \text{ \AA}, \quad (14)$$

a value too small for all practical purposes unless one wants to displace atoms.

## 4 Inhomogeneous systems: cycles

Despite its robustness, the analysis in the previous section does not apply to the phenomena of interest here, *i.e.* Marangoni-driven engines. The goal of the present section is to prove this point and to develop a quantitative framework for understanding this new class of systems.

Before considering interfacial phenomena, let us appeal to a more familiar ‘pressure–volume’ paradigm. For an inhomogeneous extended system the pressure  $p(\mathbf{x})$  varies from point to point  $\mathbf{x}$ , so that the internal energy reads

$$U = TS - \int_V p(\mathbf{x}) dV_{\mathbf{x}}, \quad (15)$$

instead of  $U = TS - pV$  for homogeneous systems. The first question is how to understand the corresponding thermodynamic cycles. Plots in the  $(p, V)$ -plane seem to be no longer relevant as, for example, the average pressure  $\langle p \rangle$  could be constant thus resulting in no work done in the context of the  $(p, V)$ -diagram of Fig. 7 if the system is treated as homogeneous with the  $p$ -axis being simply  $\langle p \rangle$ . However, it is clear that an inhomogeneous pressure distribution with the same average should result in non-zero energy storage, which if properly harnessed can be used to perform work. In the same way, for the interfacial system<sup>||</sup>

$$U = TS + \int_A \sigma(\mathbf{x}) dA_{\mathbf{x}}, \quad (16)$$

the diagram in the  $(\sigma, A)$  plane with  $\sigma$  understood as the average (over the entire system) value  $\langle \sigma \rangle$  would result in zero work done if  $\langle \sigma \rangle = \text{const}$  even if the interfacial area  $A$  experiences non-negligible variation since the integral  $\int \langle \sigma \rangle dA$  is zero over the cycle.

To develop intuition about energy storage in such inhomogeneous systems, let us first appeal to a basic mechanical example – a longitudinally distorted elastica, *cf.* Fig. 9. If the longitudinal distortion of an elastica is described by a function  $\xi(x, t)$ , then the left edge of a segment  $\Delta x$  at some time instant  $t$  is displaced from its undisturbed position through distance  $\xi(x, t)$  and the right edge through distance  $\xi(x + \Delta x, t)$  as shown

<sup>||</sup> It is important to contrast the sign difference between  $+\sigma A$  and  $-pV$  in the expression (15) – both represent the work done on the system: in the latter if  $dV < 0$  the work is positive, while in the former one needs to increase the area  $dA > 0$  to increase the energy of the system.

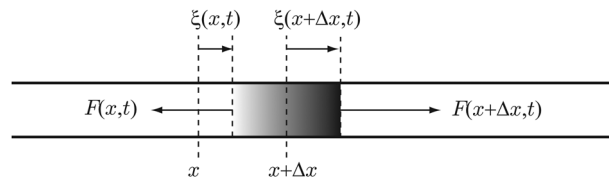


Fig. 9 Longitudinally distorted elastica: displacement and deformation of an elastica segment  $\Delta x$  caused by a longitudinal wave  $\xi(x, t)$  at some time instant  $t$  and the forces  $F(x, t)$  and  $F(x + \Delta x, t)$  exerted on the edges of the segment.

in Fig. 9. The elastic force  $F(x, t)$  of interaction between adjoining segments of the stretched elastica consists of a constant tension  $T$  (which could be present when the elastica is not distorted yet) and an additional part related to a non-uniform distortion. According to Hook’s law,

$$\begin{aligned} F(x, t) &\approx T + SY \frac{\xi(x + \Delta x) - \xi(x)}{\Delta x_0} \\ &\approx T + (SY + T) \frac{\partial \xi(x, t)}{\partial x}, \end{aligned} \quad (17)$$

where  $Y$  is Young’s modulus of the elastica material,  $S$  the cross-sectional area of the elastica, and we took into account that the equilibrium length  $\Delta x_0$  of the segment is related to the deformed one  $\Delta x$  via  $\Delta x = \Delta x_0(1 + T/SY)$ . Hence, the net force  $\Delta F$  exerted on the segment  $\Delta x$  by its neighbors becomes

$$\begin{aligned} \Delta F(x, t) &\approx (SY + T) \left[ \frac{\partial \xi(x + \Delta x, t)}{\partial x} - \frac{\partial \xi(x, t)}{\partial x} \right] \\ &\approx (SY + T) \frac{\partial^2 \xi(x, t)}{\partial x^2} \Delta x, \end{aligned} \quad (18)$$

The work done by this external longitudinal force while the segment  $\Delta x$  moves to its new position  $\xi(x, t)$  is

$$\Delta W = -\frac{1}{2}(SY + T) \xi \frac{\partial^2 \xi(x, t)}{\partial x^2} \Delta x. \quad (19)$$

The total potential energy of the deformation created by this work over the entire elastica becomes after integration by parts

$$E_{\text{pot}} = \frac{1}{2}(SY + T) \int_a^b \left( \frac{\partial \xi(x, t)}{\partial x} \right)^2 dx, \quad (20)$$

where we considered the endpoints  $a$  and  $b$  of the elastica fixed. Hence, even if the elastica is initially under zero tension,  $T = 0$ , the potential energy is non-zero. As we will show below, a similar argument can be applied to the energy storage by a fluid due to bulk compressibility (Sections 4.1 and 4.2) and then by the fluid interface due to its compressibility (stretchability) even if the bulk flow is incompressible (Section 4.3).

### 4.1 Pressure-gradient driven two-degree of freedom system

Let us consider a simple two-degree of freedom system as a first approximation of an infinite-dimensional distributed one – two ideal gases of equal amounts and at an equal temperature  $T_0$  separated by an insulating divider and contained in a thermally insulated cylinder – as shown in Fig. 10. Despite its simplicity, this

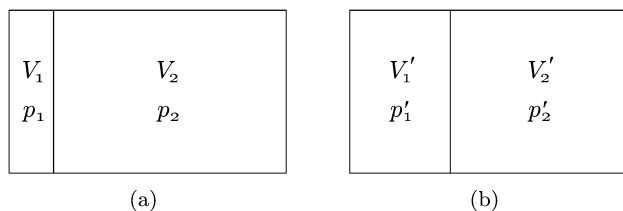


**Fig. 10** A gas-piston system of two ideal gases of masses  $m_1$  and  $m_2$ . (a) Initial state at  $t = 0$  with uniform temperature  $T_0$ . (b) Final state with  $p_1' = p_2'$  and  $T_1' \neq T_2'$  settles after some oscillations of the divider due to elasticity of the ideal gas.

system will be instrumental for understanding inhomogeneous systems in terms of thermodynamic cycles. Clearly,  $p_1/p_2 = V_2/V_1$  as follows from the ideal gas equation of state,  $pV = mRT$ , where  $R$  is the gas constant. Intuitively, the smaller the ratio  $V_1/V_2$ , the more energy one can extract from this piston-cylinder system by harnessing the moving divider to a work performing mechanism.

Assuming, for simplicity, that the process is fast and hence can be approximated as adiabatic (similar to how sound wavepacket propagation through air is fast enough so that no appreciable heat exchange takes place<sup>68</sup>), we immediately conclude that equilibrium thermodynamics only allows us to determine the final pressure, which must equilibrate in both chambers to

$$p = \frac{p_1 V_1 + p_2 V_2}{V_1 + V_2}. \quad (21)$$

The above equation is the consequence of the total internal energy conservation  $U_1 + U_2 = U_1' + U_2'$ , *i.e.* before and after the divider is released, since the work performed by one gas on the other is converted into the internal energy change of each gas; here we also took into account that the internal energy of the ideal gas is a function of temperature only,  $U = c_v T = (pV)/(\gamma - 1)$ , where  $\gamma = c_p/c_v$ . The final position of the divider cannot be found in the framework of equilibrium thermodynamics.<sup>69</sup> The only other conclusion one can make is that the thermally insulated amounts of gas will have their temperature changed to unequal values and both entropies increased,  $\Delta S_{1,2} > 0$ , thus indicating irreversibility of the process (the potential energy of the compressed gas in the left chamber went into both configurational and dissipative work).

Even in the case of a quasi-static process (*i.e.* infinitely slow, which can be achieved by taking the divider infinitely heavy), so that  $pV^\gamma = \text{const}$  in each chamber, neglecting the heat capacities of the container and the divider, we readily find that the volume  $V_1$  occupied by the left gas changes to  $V_1'$  determined by

$$\frac{V_1}{V_1'} = \frac{V_1}{V_2} \frac{1 + \left(\frac{V_1}{V_2}\right)^{\frac{1}{\gamma}-1}}{1 + \frac{V_1}{V_2}}, \quad (22)$$

and  $V_2'$  follows from the volume conservation,  $V_1 + V_2 = V_1' + V_2'$ . Since there is no heat exchange with surroundings, the work done is equal to the internal energy change

$$\Delta U_i = m_i c_v (T_i' - T_0), \quad (23)$$

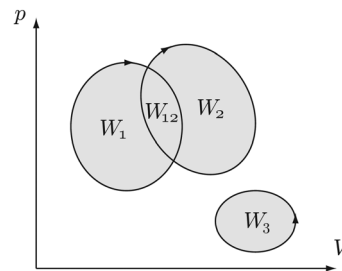


**Fig. 11** A thermodynamic cycle for a three-degree of freedom system. The total work done is  $W_{\text{total}} = W_1 + W_2 - W_{12} - W_3$ .

where  $T_i'/T_0 = (V_i/V_0)^{\gamma-1}$ . From the resulting expression one can clearly see that the resulting temperature distribution becomes non-uniform, *i.e.* both gases acquire different temperatures despite the same initial temperature and reversibility of the quasi-static process (only configurational work is performed in this case).

Most importantly, this system gives an idea how to understand a thermodynamic cycle of a many degree of freedom system, including infinite-dimensional, in the  $(p, V)$ -space: namely, each fluid parcel (*i.e.* infinitely small element<sup>70</sup> compared to the volume of the system under consideration, but large compared to the distance between the molecules) has its own cycle as that in Fig. 7, which may produce either positive or negative total work – the superposition of all these cycles (an infinite number of them, in fact, for an extended system) gives the resulting work done by the entire system consisting of an infinite number of such parcels. Fig. 11 illustrates a motor with three parcels.

Thus, the key conclusions from the finite-degree of freedom systems are that inhomogeneities generate inhomogeneities, *e.g.* an initially non-uniform pressure may lead to a non-uniform temperature distribution, and that the way to represent thermodynamic cycles of distributed systems in the  $(p, V)$ -coordinates is by treating each fluid parcel as having its own cycle.

## 4.2 Pressure-gradient driven infinite-dimensional system

Next let us consider a simple example of an infinite-dimensional (distributed) system, in which energy is stored by a non-uniform distribution of pressure inside the system volume. While pressure itself gives rise to a force  $p dA$  as in the example considered in Section 4.1 above, the pressure gradient is also a force as can be seen from the momentum equation of fluid motion, namely acceleration of a unit mass is  $du/dt \sim -\rho^{-1} \nabla p$ . Hence, the elementary force acting on an elementary volume  $dV$  is  $dF = \nabla p dV$ , and thus its work over an elementary directed path  $ds$  is

$$dF \cdot ds = dp dV. \quad (24)$$

To proceed with further calculation we need to assume certain equation of state, *e.g.*  $pdV = p_0 dV_0 = \text{const}$ , which is an ideal gas law applied to an elementary fluid parcel of initial size  $dV_0$  under constant temperature. From the fundamental thermodynamic relationship we find that under constant temperature  $dU - T dS = d(U - TS) = dF = -pdV$ , *i.e.* the elementary Helmholtz free energy  $dF$  of a fluid parcel is preserved during a parcel deformation. The Helmholtz free energy  $F$  naturally appears here as a thermodynamic potential minimized under

constant temperature and volume. However, we can talk about thermodynamic properties of a fluid parcel only since the entire system is not in thermodynamic equilibrium, *e.g.* due to pressure changing from parcel to parcel. With such an understanding of the equation of state, an elementary work done on the initially homogeneous system at pressure  $p_0$  is then

$$\delta W = \int d\mathbf{F} \cdot d\mathbf{s} = \int_{p_0}^p dp dV = p_0 dV_0 \int_{p_0}^p \frac{dp}{p}, \quad (25)$$

which is positive if  $dp > 0$  since here  $dV$  stands for the parcel volume, which cannot become negative. The total work  $W = \int \delta W$  performed on the system is

$$W = \int_V p dV \int_{p_0}^p \frac{dp}{p} = \int_V p(\mathbf{x}) \ln \frac{p(\mathbf{x})}{p_0} dV_{\mathbf{x}}, \quad (26)$$

where we used the equation of state  $dV_0 = (p/p_0)dV$  in order to integrate over the final volume  $V$  with the goal to evaluate the stored energy distribution due to the pressure non-uniformities in the final state. The argument  $\mathbf{x}$  in (26) indicates the dependence of pressure on the location  $\mathbf{x}$  inside the volume  $V$ . Since for an ideal gas under constant temperature the change in the internal energy is zero,  $dU = 0$ , which is because the internal energy of an ideal gas is a function of temperature only, then from (1) all the work must be compensated by the heat,  $\delta W = -\delta Q$ . The latter means that  $S \sim -W$  and hence, from the expression (26), it follows that the entropy is a sum of  $p(\mathbf{x}) \ln(p(\mathbf{x})/p_0)$  over all elementary volumes, which is Shannon's entropy<sup>71</sup> – a generalization of Boltzmann's formula for entropy to the case when microstates do not have equal probability. That is, the meaning of (26) is the computation of all possible permutations over all possible elementary volume deformations modulo the identical ones.

Obviously, the work (26) done by the pressure gradient forces is different from that done by the pressure force  $\int p dV$  on a homogeneous system, *i.e.* in which  $p$  is the same everywhere and  $dV$  means the change in the total volume of the system. In (26), since  $p_0$  is the initial uniform distribution in our case, it is impossible to have  $p/p_0 > e$  pointwise everywhere if the total volume of the system stayed unchanged as in the example discussed in Section 4.1 – hence it is impossible to overperform  $\int p dV$ , which is the available expansion energy if the work is done in an isentropic expansion as discussed below. In this respect, one may also ask what is the difference between the work done (26) from the functional  $\int p(\mathbf{x}) dV_{\mathbf{x}}$  in (15), where the index  $\mathbf{x}$  shows that pressure depends on a point  $\mathbf{x}$  in the volume? During a reversible isentropic process  $dS = 0$ , the latter functional representing the work of pressure forces is converted into internal energy based on the first law (1):  $dU = TdS - pdV = -pdV$ , which means that the process is adiabatic, in contrast to the condition of the isothermality assumed in the derivation of (26). Eqn (26), when applied to an ideal gas as we observed above, implies that all the work is converted instead into heat as the internal energy does not vary under constant temperature. Of course, one may also consider the functional  $\int p(\mathbf{x}) dV_{\mathbf{x}}$  as interpreted in an irreversible process, say, free expansion where the work done  $\delta W$  is zero, but the integral  $\int p dV$  is not; also, while the heat generated is zero  $\delta Q = 0$ , there is

certainly an increase in entropy. In the case of an ideal gas, the internal energy change  $dU = 0$ , which means that the temperature  $T$  does not change, but because  $dU = TdS - pdV$  is still valid since it relates the state variables, then apparently  $\int p dV$  is converted into the increase of the entropy  $T \int dS$ .

### 4.3 Surface tension-gradient driven system

Now, turning our attention to systems with interfaces, we note that the internal energy of the interface  $U_s$  is given by the fundamental thermodynamic relationship<sup>72</sup>

$$dU^s = TdS^s + \sigma dA + \sum_i \mu_i dN_i^s, \quad (27)$$

where  $S^s$  and  $N^s$  are interfacial entropy and number of particles/molecules, respectively. Applying Euler's homogeneous function theorem to (27) we find the corresponding Euler's integral

$$U^s = TS^s + \sigma A + \sum_i \mu_i N_i^s. \quad (28)$$

Generalizing this functional to a distributed system with a surface tension variation  $\sigma(\mathbf{x})$  along the interface we get

$$U^s = TS^s + \int_A \sigma(\mathbf{x}) dA + \sum_i \mu_i N_i^s, \quad (29)$$

*i.e.* eqn (16) with the presence of several chemical components taken into account. The question now is how this spatial inhomogeneity of  $\sigma(\mathbf{x})$  affects the energy that can be extracted from a system. For example, it is clear that if one starts with a spherical drop uniformly covered with a surfactant, it takes work to redistribute surfactant non-uniformly along the drop surface.

To address this question, consider the dynamic boundary condition at the interface (without surface viscosities)

$$\mathbf{T} \cdot \mathbf{n} = \nabla_s \cdot (\mathbf{I}_s \sigma) = 2H\sigma \mathbf{n} + \nabla_s \sigma, \quad (30)$$

where  $T_{ij} = -p\delta_{ij} + \tau_{ij}$  is the complete stress tensor,  $s$  the arclength,  $\nabla_s$  surface gradient,  $\tau_{ij}$  viscous stress tensor,  $\mathbf{n}$  the normal vector,  $\mathbf{I}_s$  surface idemfactor, and  $H = -\nabla_s \cdot \mathbf{n}/2$  the mean curvature. After a projection of (30) onto the tangent vector  $\mathbf{t}$  we get the balance of viscous and Marangoni stresses:

$$\mathbf{t} \cdot \tau \cdot \mathbf{n} = -\mathbf{t} \cdot \nabla_s \sigma = \partial_s \sigma, \quad (31)$$

*i.e.* without the bulk viscosity, so that  $\tau = 0$ , the Marangoni stresses cannot be physically present<sup>70</sup> – this observation will be crucial later on. To determine an elementary force acting on the elementary oriented area  $d\mathbf{A} = \mathbf{n}dA$  of the interface, *cf.* Fig. 12, recall that the stress-tensor is defined as  $\tau_{ij} = \delta F_j / \delta A_i$ , so that the force becomes  $dF_i = \tau_{ij} dA_j = \tau_{ij} n_j dA = (\nabla_s \sigma)_i dA$ , and hence the work done to modify the element  $dA_0$  into  $dA$  with the surface surfactant concentration changing from  $\Gamma_0$  to  $\Gamma$  over an elementary path  $d\mathbf{s} = \mathbf{t}ds$  is\*\*

$$\delta W = - \int d\mathbf{F} \cdot d\mathbf{s} = - \int d\sigma dA. \quad (32)$$

\*\* Clearly, if  $dA_0 = dA$  and hence  $\Gamma_0 = \Gamma$  provided  $\Gamma dA = \Gamma_0 dA_0$ , then there is no surface tension gradient and thus the work done  $dW = 0$ .

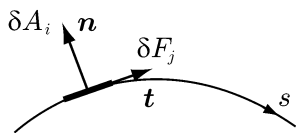


Fig. 12 On the stress-tensor definition.

Expression (32) in contrast to (25) has a negative sign because this is the work done against Marangoni stresses<sup>††</sup> if the interface is locally shrunk, *i.e.* when surfactant concentration  $\Gamma$  is locally increased,  $d\Gamma > 0$ , so that surface tension  $\sigma$  decreases,  $d\sigma < 0$ , and hence acts against the interface shrinkage; note that  $dA > 0$  as a given surface element cannot shrink to a negative value. If  $\Gamma dA = \Gamma_0 dA_0$  is a local conservation<sup>‡‡</sup> of the surfactant surface concentration  $\Gamma$  for a surface element (in the integral form  $\int_A \Gamma dA$ ) valid for insoluble monolayer or when the interface deformations are much faster compared to the sorption kinetic time scales, then

$$\delta W = -\Gamma_0 dA_0 \int_{\Gamma_0}^{\Gamma} \sigma'(\Gamma) \frac{d\Gamma}{\Gamma}, \quad (33)$$

where  $\sigma'(\Gamma) = d\sigma/d\Gamma$  and we used the assumed surfactant amount conservation  $dA_0 = (\Gamma/\Gamma_0)dA$ . For example, if the surface tension is a linear function of concentration,  $\sigma = \sigma_0 - K\Gamma$  with  $K > 0$ , then (33) gives

$$\delta W(\mathbf{x}) = K\Gamma(\mathbf{x}) \ln \frac{\Gamma(\mathbf{x})}{\Gamma_0} dA(\mathbf{x}), \quad (34)$$

where we assigned an index  $\mathbf{x}$  to each elementary area  $dA(\mathbf{x})$  as it is stretched differently at different locations  $\mathbf{x}$ . Formula (34) was formally derived earlier by Schwartz and Roy,<sup>73</sup> but without further insights into its meaning and out of the context of thermodynamics, which will be addressed in Section 5.1. Similar to the interpretation of formula (26) in terms of Shannon's entropy, one can apply the analogous argument to (34) – in the case of the linear surface equation of state the elementary work (33) is just a computation of permutations of all possible deformations of elementary surface elements modulo the identical ones thus leading to (34) and for the general equation of state it modifies the distribution of probability with the weight  $\sigma'(\Gamma)$ , *cf.* eqn (33). Note that in the derivation of the work (32) we took into account only the work done against Marangoni stresses, but not the work of creating inhomogeneities in chemical energy – the last term in (27) – which is justified by the assumed surfactant mass conservation so that  $dN^s = 0$ . In general, however, the expression for the work required for creating inhomogeneities should account for variations of both surface tension and chemical potential along the interface.

The total amount of work done on the system is found after summing up over all elementary transformed areas  $dA$ 's, *i.e.*

<sup>††</sup> A good analogy would be the work of pushing a block of weight  $mg$  along a surface against friction forces  $\mu mg$ :  $dW = -\mathbf{F} \cdot d\mathbf{s} = \mu mg ds$ , where  $\mathbf{F} = -\mu mg$  as this force must, at least, balance the friction force.

<sup>‡‡</sup> Note that *versus* this local conservation law, the global one for uniform distribution of surfactant would state  $\Gamma A = \text{const}$ , which in turn implies that when either the area or concentration changes (uniformly), then  $dA = -A d\Gamma/\Gamma$ .

after integration over the final state area  $A$ , which gives the total energy of a particular surfactant configuration:

$$W = \int \delta W = -\int_A \Gamma \int_{\Gamma_0}^{\Gamma} \sigma'(\tilde{\Gamma}) \frac{d\tilde{\Gamma}}{\tilde{\Gamma}} dA, \quad (35)$$

or the work (stored energy) density per unit area

$$\frac{\delta W}{\delta A} = -\Gamma \int_{\Gamma_0}^{\Gamma} \sigma'(\tilde{\Gamma}) \frac{d\tilde{\Gamma}}{\tilde{\Gamma}}. \quad (36)$$

For example, if the interface is shrunk everywhere, then  $\Gamma > \Gamma_0$ , but since  $\sigma'(\Gamma) < 0$ ,  $\delta W/\delta A$  is positive. Note that the work done in (35) is path-independent in the sense that it does not depend on the manner in which the surfactant distribution was achieved – this is due to the fact that the reactive force is a gradient of a potential function (surface tension), but expression (36) depends on the material behavior  $\sigma'(\Gamma)$ ; in fact,  $W > 0$  as the standard interfacial material behavior obeys  $\sigma'(\Gamma) \leq 0$ . In this sense, in the general formula (35) there is dependence on the gradient of the concentration  $\Gamma$ , even though it is implicit, as opposed to the interpretation of Schwartz and Roy.<sup>73</sup>

It is straightforward to show that (35) is always non-negative under the constraint that the total amount of surfactant is conserved, *i.e.*  $\int_A \Gamma dA = \text{const}$ . First, one can consider the case of constant  $\sigma'(\Gamma)$ , which reduces the problem to variational one with a constraint, *e.g.* for simplicity when the area  $A$  is an interval of length  $l$

$$I(f) = \int_0^l f \ln f dx, \quad \frac{1}{l} \int_0^l f dx = 1. \quad (37)$$

The minimum  $I(f) = 0$  is achieved at  $f = 1$  and the corresponding Lagrange multiplier  $\lambda = l$ . For all other distributions of  $f$ ,  $I(f) > 0$ . Next, noting that  $\sigma'(\Gamma)$  is sign-definite, one can majorize the integral in (35) and thus prove that  $W \geq 0$  for general material behavior  $\sigma'(\Gamma)$ . From (37) it is clear that  $f$  behaves as a probability distribution function on the unit interval  $x/l \in [0, 1]$ .

In summary, as opposed to moving a block along a surface against the friction force, in which case the work spent on pushing does not lead to energy storage, in the case of Marangoni stress despite its inevitable coupling to the bulk shear and thus bulk dissipation (31), not all work against Marangoni stresses is converted into kinetic energy of dragged fluid and viscous dissipation at the same rate as the work is performed, which allows for energy storage and subsequent release. This is similar to compressing an elastica as discussed at the beginning of this section, which also has some dissipation in the process of deformation, but nevertheless stores some energy. From a practical point of view, if the elastica remains the same length as its undeformed state, then such a potential energy is usually considered useless unless the resulting longitudinal waves propagating in the string<sup>74</sup> are harnessed to be converted into non-expansion work (*e.g.* shaft work, stirring, *etc.*) and eventually into heat. In our case, however, the boundary condition (31) coupling viscous and Marangoni stresses allows for energy extraction from the inhomogeneity in surface tension, which can be used, for example, for stirring, as the bulk fluid is dragged by Marangoni gradients at the interface.

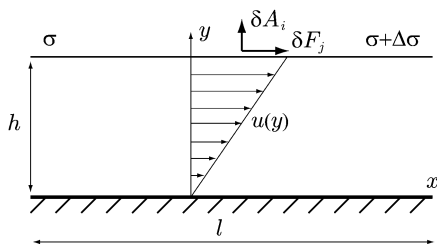


Fig. 13 Marangoni effects in a thin film.

#### 4.4 Thin film

As a particular case of application of (35), let us consider a thin film with a non-uniform distribution of an insoluble surfactant, cf. Fig. 13.

The corresponding initial-boundary value problem for the plane-parallel case (no vertical velocity component and no free surface deformation) reads

$$\frac{\partial u}{\partial x} + \frac{\partial v}{\partial y} = 0, \quad (38a)$$

$$\frac{\partial u}{\partial t} + u \frac{\partial u}{\partial x} = -\frac{1}{\rho} \frac{\partial p}{\partial x} + \frac{\mu}{\rho} \left( \frac{\partial^2 u}{\partial x^2} + \frac{\partial^2 u}{\partial y^2} \right), \quad (38b)$$

$$\frac{\partial \Gamma}{\partial t} + \frac{\partial}{\partial x} (\Gamma u_s) = D \frac{\partial^2 \Gamma}{\partial x^2}, \quad (38c)$$

$$y = 0: u = 0, \quad (38d)$$

$$y = h: \mu \frac{\partial u_s}{\partial y} = \frac{d\sigma}{d\Gamma} \frac{\partial \Gamma}{\partial x}, \quad (38e)$$

where the latter boundary condition corresponds to (31) with the force component being  $\delta F_x$  and the oriented area  $\delta A_y$ , cf. Fig. 12 and 13, so that  $\tau_{yx} = \delta F_x / \delta A_y = \mu du/dy$ . In (38b) we crossed out the vanishing terms: velocity  $u$  is no longer a function of  $x$  thanks to the continuity eqn (38a) – if  $u_x \neq 0$ , then there would be a non-zero vertical velocity component; also there is no externally imposed pressure gradient  $p_x = 0$ . It is easy to see that the above system admits the following exact solution for the surfactant concentration and the fluid velocity, respectively:

$$\Gamma(t, x) = -\frac{\sigma'}{\mu} \alpha^2 h t + \Gamma_0(x), \quad u(y) = \frac{\sigma'}{\mu} \alpha y, \quad (39)$$

where we denoted  $\sigma' \equiv d\sigma/d\Gamma$  and  $\Gamma_0(x) = \alpha x$  is the initial surfactant concentration distribution. Clearly, the flow is driven by the concentration gradient, i.e. if  $\alpha = 0$  then there is no induced fluid motion. Multiplying (38b) by  $u$  and integrating across the film we find the rate of fluid kinetic energy change (dropping the factor  $\mu/\rho$ ) for the steady-state (fully developed) velocity profile (39)

$$\int_0^h u \frac{\partial^2 u}{\partial y^2} dy = \underbrace{u \frac{\partial u}{\partial y} \Big|_0^h}_{\text{energy input}} - \underbrace{\int_0^h \left( \frac{\partial u}{\partial y} \right)^2 dy}_{\text{dissipation}} = 0, \quad (40)$$

where both energy input and dissipation are equal to  $(\sigma' \alpha / \mu)^2 h$  and thus cancel each other, i.e. the energy input due to the

surfactant concentration  $\Gamma(x)$  gradient is balanced by viscous dissipation. As it was mentioned above, the presence of dissipation is unavoidable in Marangoni-driven systems, which can be seen from eqn (31) – existence of Marangoni stresses implies the presence of viscosity.

#### 4.5 Effects of surfactant solubility

To account for the effect of surfactant solubility, for transparency let us again consider a film of thickness  $h$ , which is being manipulated to achieve a non-uniform distribution of surfactant and hence capable of delivering energy. Local mass balance in this case reads

$$(Ch + \Gamma) dA = (C_0 h + \Gamma_0) dA_0, \quad (41)$$

where  $C$  is the bulk concentration. For the purpose of our analysis and the points to be made it is sufficient to limit ourselves to Henry's equilibrium isotherm, i.e.  $\Gamma = K_H C$ . First consider the case when the film thickness does not change in the process, which leads to

$$(h/K_H + 1) \Gamma dA = (h/K_H + 1) \Gamma_0 dA_0, \quad (42)$$

but because the factor  $(h/K_H + 1)$  stays constant, this case is reduced to that already considered in Section 4.4, i.e. when the surfactant is treated as insoluble,  $\Gamma dA = \Gamma_0 dA_0$ . Therefore, it is more interesting to treat the case of variable film thickness, e.g. when due to fluid incompressibility the film volume is conserved, which implies that  $dV = h dA = \text{const}$ . In this case the local surfactant conservation law reads

$$CdV + \Gamma dA = C_0 dV_0 + \Gamma_0 dA_0. \quad (43)$$

Hence, one can decompose the work into two integrals – the first over the interface  $W_s$ , which has already been considered (35), and the second over the bulk  $W_b$  following the same procedure as in deriving (35):

$$W_b = - \int_V C \int_{C_0}^C \sigma'(C) \frac{dC}{C} dV, \quad (44)$$

where now we consider surface tension as a function of the bulk concentration (in any case  $C$  and  $\Gamma$  are related by the Henry isotherm). Since  $\sigma'(C) < 0$ , the work  $W_b$  is positive, which suggests energy storage in the bulk. Physically, this is straightforward to appreciate: let the redistribution of surfactant in a non-uniform concentration state happens slowly enough (or the film to be thin enough for the processes of diffusion and sorption to happen fast) so that the equilibration between the bulk and surface concentrations is achieved, but fast enough to avoid the bulk diffusion along the film extent bringing the entire system to a uniform equilibrium at each location along the film, cf. Fig. 14a. Then, when the film is released to perform work it happens on a time scale faster than that required for achieving an equilibrium between the bulk and surface concentrations – in this case, the first part of the work is initially performed by the surfactant at the interface alone (Fig. 14a) and then, once the bulk concentration exchanges with the interface (Fig. 14b) producing a new non-uniformity of the

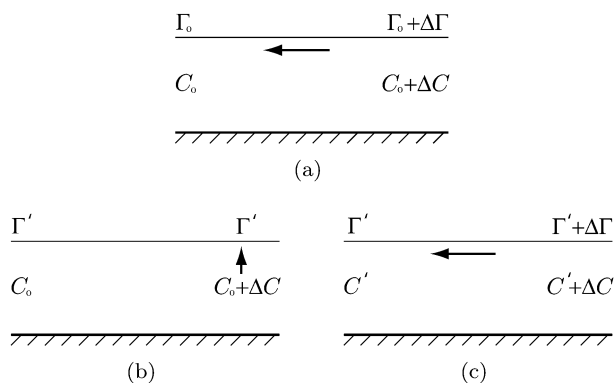


Fig. 14 On the Marangoni flow in a soluble surfactant-laden film. (a) Step 1: interfacial concentration induced Marangoni flow. (b) Step 2: excess bulk surfactant is supplied to the interface. (c) Step 3: final  $\Gamma$ -induced Marangoni flow.

surface concentration (Fig. 14c), it leads to an extra work  $W_b$  performed.

Finally, it is worth commenting on the case when time-dependence of the surfactant kinetics is comparable to the engine operation time scale. Let us consider the case of the non-equilibrium Henry isotherm, which will be sufficient for our purposes:

$$\frac{d\Gamma}{dt} = k^a C(t) - k^d \Gamma(t), \quad (45)$$

where  $k^a$  and  $k^d$  are the adsorption and desorption coefficients, respectively. Obviously, in this case  $\Gamma dA \neq \Gamma_0 dA_0$  and, because of the time-dependence, it makes sense to focus on the power production – from (32) we find:

$$\begin{aligned} P &= \frac{\delta W}{\delta t} = - \int_A \sigma'(\Gamma) \frac{d\Gamma}{dt} dA \\ &= - \int_A \sigma'(\Gamma) [k^a C(t) - k^d \Gamma(t)] dA, \end{aligned} \quad (46)$$

or simply power density per unit area

$$\frac{\delta P}{\delta A} = -\sigma'(\Gamma) [k^a C(t) - k^d \Gamma(t)], \quad (47)$$

which by comparing with the work density (36) in the time-independent case suggests that the first term in (47) – adsorption of surfactant from the bulk to the interface in step 2 of Fig. 14b – contributes to increasing power (recall that  $\sigma'(\Gamma) \leq 0$ ), while the last one – desorption of surfactant from the interface to the bulk – decreases the delivered power.

#### 4.6 Period of a Marangoni-driven cycle

Appealing again to the case of a thin film of thickness  $h$  with a non-uniform distribution of an insoluble surfactant (or when sorption is slow) over an area of size  $l$  as shown in Fig. 13, we can estimate the period of a Marangoni-driven cycle. The balance of Marangoni and viscous stresses (31) gives

$$\frac{\Delta\sigma}{l} \sim \frac{\mu}{h}, \quad (48)$$

so that the time it takes to redistribute surfactant uniformly is

$$\Delta t \sim \frac{l}{u} \sim \frac{\mu}{\Delta\sigma} \frac{l^2}{h}. \quad (49)$$

For a drop,  $l \sim h$ , so that one gets  $t \sim l\mu/\Delta\sigma$ . After this time, the non-uniform surface tension distribution should be restored, as it happens in the pendant drop phenomena in Fig. 6, which repeats the cycle.

#### 4.7 The role of singularity

Singularities at a macroscopic level are crucial for reinitializing the Marangoni cycle. For example, singularity formation is instrumental in the chemical-reaction driven pendant drop<sup>75</sup> shown in Fig. 6 – tip-streaming allows for removal of surfactant from the interface giving space for production of a ‘fresh’ surfactant and hence a concentration gradient. In fact, as known from experimental observations, among the regimes of interfacial mechanical motion are violent and erratic pulsations,<sup>38–41</sup> all of which indicate intermittent formation of interfacial singularities.

With reference to Fig. 6 one can make a few further observations. First, should the concentration be the same along the interface, the chemical potential near the tip of the drop must be significantly larger because of the general curvature-dependence of the chemical potential governed by the Gibbs–Thomson equation<sup>76</sup> – hence one would expect motion from the tip (region of high  $\mu$ ) towards the base of the drop. However, in the dynamic situation the concentration near the tip due to tip-streaming is lower compared to that near the base of the drop where the fluid is not moving, which reconciles the fact that the direction of fluid motion is observed from the drop base (region of higher concentration and thus higher chemical potential) towards the tip (region of lower concentration and thus lower chemical potential). However, because the chemical potential is a function of both concentration and curvature, one would expect that due to these two competing factors there should be a critical value of the tip radius of curvature at which the process would stop.

Finally, in terms of thermodynamic cycles for distributed systems, cf. Fig. 11, it is only one parcel which is being highly deformed and torn up – hence its corresponding cycle is not closed as at some point in time it is no longer part of the system, cf. Fig. 15. This is how a singularity exhibits itself in standard thermodynamic terms.

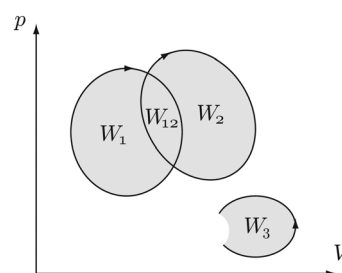


Fig. 15 A cartoon on how an interfacial singularity is reflected on a thermodynamic cycle for a three-degree of freedom system. A cycle of one of the fluid parcels is ruptured due to removal of the working fluid from the system.

## 5 Inhomogeneous systems: thermodynamics

### 5.1 Irreversibility of interfacial systems

To get a better insight into the meaning of formula (35) let us compare it with what the standard thermodynamic cycle for homogeneous systems would predict, which of course requires that the surfactant concentration is either uniformly distributed or considered in an averaged sense so that one has a global conservation law  $A\Gamma = \text{const} \equiv A_0\Gamma_0$  – the change in the surface energy  $\varepsilon_s$  for small variation in the area and hence concentration  $d\Gamma = \Gamma - \Gamma_0$  reads

$$d\varepsilon_s = A\sigma(\Gamma) - A_0\sigma(\Gamma_0) = A_0\sigma_0 \frac{d\Gamma}{\Gamma} \left[ \Gamma_0 \frac{\sigma_0'}{\sigma_0} - 1 \right], \quad (50)$$

which is negative as  $\sigma_0' \equiv \sigma'(\Gamma_0) < 0$ , *i.e.* the energy decreases if the interface is compressed and thus the concentration is increased,  $d\Gamma > 0$ . This, from a first glance, counterintuitive result is, however, expectable since both  $A_0$  and  $\Gamma_0$  are larger than their final values  $A$  and  $\Gamma$ , but certainly contradicts (35), *i.e.* the fact that energy can be extracted if the interface is contracted as predicted by the analysis of the system when treated as inhomogeneous one.

First, the negative sign of (50) suggests that, according to the principle of minimum energy, the interface can shrink to zero area on its own, but in practice this is impossible because the volume enclosed by the interface cannot be compressed indefinitely plus there are effects of external forces such as gravity, which prevent liquids from assuming the minimal spherical shape.

Second, to make the contrast of (50) with what formula (35) would predict more transparent, consider the case when both the initial and final states have a uniform surfactant distribution (otherwise (35) should be integrated over  $A(\mathbf{x})$  and  $d\Gamma(\mathbf{x})$ ), *e.g.* when  $\sigma'(\Gamma) = -K = \text{const}$ :

$$W = K\Gamma \ln \frac{\Gamma}{\Gamma_0} A, \quad (51)$$

which is positive if the final concentration  $\Gamma$  is higher than the initial one  $\Gamma_0$ , *i.e.* if the final area  $A < A_0$  even if the initial  $\Gamma_0$  and final  $\Gamma$  surface concentrations are both uniform – notably this is in contrast to (50) obtained without accounting for the physics of Marangoni effects, which act in the process leading from an initial to a final state. One could argue that one can get from such an initial to final state quasi-statically so that at each infinitesimal step  $\Gamma = \text{const}$ . However, obviously this is impossible as it would require in the process of interface shrinking to control each of the surfactant molecules individually to make sure that they are equidistant from each other – similar to Maxwell's demon<sup>77</sup> it would require a non-zero work to be done.

Finally, note that since (50) corresponds to the term  $\sigma dA$  in the energy balance (27) and does not account for the work done against Marangoni stresses (32), then eqn (27) also does not account for the physics of energy storage/production on surface tension inhomogeneities. Basically, elementary work (32) in a distributed system is not part of (27) for a homogeneous system – the latter is written for the change of the entire system, while the

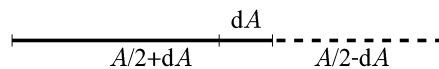


Fig. 16 On asymmetry and irreversibility of interfacial changes.

former is for its elementary part. Hence one cannot simply add (32) to (27).

To see this from another point of view, let us consider the process in which half of a flat interface of constant area is being stretched by  $dA$ , while the other half is being shrunk by the same amount  $-dA$ , *cf.* Fig. 16 – overall the process conserves the total area and should be called isochoric in analogy with the isochoric, *i.e.* constant-volume, process. §§ Assuming that the surfactant is uniformly distributed in the process, the change in the surface energy in this case, *e.g.* for the right half, is

$$\begin{aligned} d\varepsilon_s^r &= \sigma(\Gamma + d\Gamma)(A - dA) - \sigma(\Gamma)A \\ &= \sigma_\Gamma(\Gamma)\Gamma dA + \sigma_{\Gamma\Gamma}(\Gamma)\Gamma^2 \frac{(dA)^2}{2A} + \text{h.o.t.}, \end{aligned} \quad (52)$$

where we took into account that

$$\frac{d\Gamma}{\Gamma} = \frac{dA}{A} + \left( \frac{dA}{A} \right)^2 + \dots \quad (53)$$

The surface energy change  $d\varepsilon_s^l$  for the left half follows from the change of signs,  $dA \rightarrow -dA$  and  $d\Gamma \rightarrow -d\Gamma$  in (52):

$$\begin{aligned} d\varepsilon_s^l &= \sigma(\Gamma + d\Gamma)(A - dA) - \sigma(\Gamma)A \\ &= \sigma_\Gamma(\Gamma)\Gamma dA + \sigma_{\Gamma\Gamma}(\Gamma)\Gamma^2 \frac{(dA)^2}{2A} + \text{h.o.t.} \end{aligned} \quad (54)$$

Clearly, as opposed to the clean interface case when  $\sigma = \text{const}$ , the energies  $d\varepsilon_s^r$  and  $d\varepsilon_s^l$  are not balanced, *i.e.* there is a positive energy produced:

$$d\varepsilon_s = d\varepsilon_s^l + d\varepsilon_s^r = \sigma_{\Gamma\Gamma}(\Gamma)\Gamma^2 \frac{(dA)^2}{A}, \quad (55)$$

so that  $\sigma_{\Gamma\Gamma}$  is an indicator of an irreversibility here. Indeed, if the process of stretching the interface and then shrinking it back is not done quasistatically, then similar to the process of compressing–decompressing ideal gas (regardless if the process is adiabatic<sup>78</sup> or isothermal<sup>79</sup>) the irreversibility is inevitable: the heat generated in the process of shrinking, *cf.* Section 5.2, is irreversibly lost to the bulk and surroundings. In fact such an irreversible behavior should not be surprising ¶¶ as the surfactant laden interface behaves as a 2D ideal gas with the equation of state for the surface pressure<sup>80</sup>  $\pi \equiv \sigma(\Gamma = 0) - \sigma(\Gamma) = RT\Gamma$  – hence the argument developed for the ideal gas in Section 4.1 applies here as well; deviations of the interface

§§ The term “isochoric” is derived from Greek *isos* meaning *equal* and *choros* meaning *space* – in analogy one can construct “isocric” from *chros* meaning *surface* of a body.

¶¶ Mathematically, this asymmetry follows from the second order differential being positive definite for any function  $f(\Gamma)$ :

$$f(\Gamma + d\Gamma) = f(\Gamma) \pm f'(\Gamma)d\Gamma + f''(\Gamma)\frac{(d\Gamma)^2}{2} + \dots \quad (56)$$

from the ideal gas law for elevated surfactant concentrations only make the irreversibility worse by increasing dissipation. The same observation of irreversibility can be made about the temperature dependence of surface tension: as known from Kelvin's calculations (see Section 5.2), when stretching the interface its temperature drops and when shrinking the interface its temperature increases, but in the process of first stretching and then shrinking by the same amount there will be irreversible changes in the system.

## 5.2 Surface entropy

As follows from (28), when  $d(\sigma A) < 0$ ,  $dU$  can still increase due to an increase in the chemical potential  $\mu$  and the heat generation resulting from the increase in temperature in the process shrinking (since the work of Kelvin<sup>81</sup> it is known that a soap film should cool down if being stretched) and in the increase in entropy as per the following considerations.

When Kelvin considered the heat absorbed by a stretching soap film, he appealed to a Carnot cycle-type of analysis,<sup>82,83</sup> cf. Appendix A, but in the case when surface tension is a function of temperature only,  $\sigma(T)$ . In reality, however, soap films cannot exist without a surfactant and hence surface tension must be considered as a function of two variables  $\sigma(T, \Gamma)$ , temperature  $T$  and surface concentration  $\Gamma$ . Despite the 'foolproof' nature of the Carnot-type analysis,<sup>82</sup> it proves to be misleading (cf. Appendix A) and, if one wants to get the correct result, too cumbersome compared to the state variables analysis to be performed below.

Having in mind a process under constant temperature  $T$  and constant external parameters, for a system of two phases and a flat interface between them it is natural to appeal to the Helmholtz free energy  $F$ : its total value and elementary change are respectively given by

$$F = -PV + \mu N + \sigma A, \quad (57a)$$

$$dF = -PdV - SdT + \mu dN + \sigma dA, \quad (57b)$$

where we added a new extensive parameter – surface area  $A$  – into consideration (in addition to  $N, V, T$ ); the free energies of each phase are:

$$F_\alpha = -PV_\alpha + \mu N_\alpha, \quad F_\beta = -PV_\beta + \mu N_\beta. \quad (58)$$

The interfacial free energy should then be

$$F_s = F - F_\alpha - F_\beta = \sigma A + \mu N_s. \quad (59)$$

To obtain the surface entropy, we derive a surface Gibbs–Duhem equation. Using  $dF$  from (57b) and writing

$$dF_\alpha = -S_\alpha dT - PdV_\alpha + \mu dN_\alpha, \quad (60a)$$

$$dF_\beta = -S_\beta dT - PdV_\beta + \mu dN_\beta, \quad (60b)$$

we have

$$dF_s = -S_s dT + \mu dN_s + \sigma dA. \quad (61)$$

Now taking a full differential of (59) and comparing with (61), we get the surface Gibbs–Duhem equation:

$$0 = -S_s dT - Ad\sigma - N_s d\mu. \quad (62)$$

Dividing the latter expression by the interfacial area  $A$  we get a formula for the surface entropy per unit area  $s_s = S_s/A$ :

$$s_s dT = -d\sigma - \Gamma d\mu, \quad (63)$$

that is

$$s_s = \frac{dS_s}{dA} = -\frac{\partial\sigma}{\partial T} - \Gamma \frac{\partial\mu}{\partial T}. \quad (64)$$

The above expression has an extra (last) term compared to Kelvin's result<sup>81</sup>  $s_s = -\partial\sigma/\partial T$ , which is due to the presence of an adsorbed substance (surfactant) and the variation of the chemical potential with temperature. Note that in (64) while the derivative  $\sigma_T$  is negative,  $\mu_T$  is generally positive as known from experimental measurements,<sup>84</sup> which means that the heat effects represented by both terms are competing, *i.e.* if the interface is being stretched ( $dA > 0$ ):

- $\delta Q_1 = -T\sigma_T dA > 0$ , so that this heat is absorbed by the interface due to the first effect in (64);

- $\delta Q_2 = -T\Gamma\mu_T dA < 0$ , so that this heat is released by the interface due to the second effect in (64), which makes sense as the interfacial entropy must lower,  $dS_s < 0$ , as  $\Gamma$  decreases and hence the number of available microstates is reduced and the chemical potential at the interface should decrease with decreasing  $\Gamma$ .

Given (64), the entropy density gradient along the interface becomes

$$\nabla_s s_s = -\left[ \frac{\partial^2\sigma}{\partial T\partial\Gamma} + \Gamma \frac{\partial^2\mu}{\partial T\partial\Gamma} + \frac{\partial\mu}{\partial T} \right] \nabla_s \Gamma, \quad (65)$$

which must indicate that the surface entropy is higher where  $\Gamma$  is higher as a simple consequence of the fact that the surfactant concentration  $\Gamma$  increases and hence does the number of available microstates per unit area. ||| Therefore  $\sigma_{T\Gamma} + \Gamma\mu_{T\Gamma} + \mu_T < 0$ . In the context of our discussion the important implication of (64) is that the interfacial entropy density  $s_s$  increases when work is performed to compress the interface (and thus to increase the surfactant surface concentration  $\Gamma$ ).

## 5.3 Isothermality

Isothermality of interfacial engines is directly related to the heat generated or absorbed at the interface due to: interface stretching/shrinking, chemical reactions at the interface, and adsorption of surfactant to and from the bulk (which itself is an example of a chemical reaction at the interface).

While the heat generation due to interface stretching was addressed in Section 5.2, the heat generation due to a chemical reaction at the interface depends on its nature. For example, if the surfactant is produced by a chemical reaction – so-called saponification – this contributes to the energy balance: such a reaction is usually of an endothermic type, meaning that it absorbs heat from the surroundings, which is why saponification reactions are often used in fire extinguishers. Therefore, with an idea to get a general useful expression, we will instead

||| This observation should not be confused with the fact that for a given amount of substance the entropy of vapor is higher than that of liquid and the entropy of liquid is higher than that of solid.

focus on adsorption as a particular case of interfacial chemical reactions, so that the heat can be calculated as a function of surface material behavior ( $\sigma, \mu$ ).

The non-expansion work done to adsorb an amount  $d\Gamma$  of surfactant to the interface of constant area  $A$  follows from the expression for the interfacial internal energy (28):

$$\delta W = \delta[\sigma A + \mu N^s] = \left[ \frac{\partial \sigma}{\partial \Gamma} + \mu + \Gamma \frac{\partial \mu}{\partial \Gamma} \right] A d\Gamma. \quad (66)$$

Naturally, surface entropy in this process is increasing  $ds_s > 0$  as the number of microstates in increasing, which allows us to determine the amount of heat to be released by the interface to surroundings in order to maintain constant temperature:

$$\begin{aligned} \delta Q &= T ds_s = T A ds_s \\ &= - \left[ \frac{\partial^2 \sigma}{\partial T \partial \Gamma} + \frac{\partial \mu}{\partial T} + \Gamma \frac{\partial^2 \mu}{\partial T \partial \Gamma} \right] T A d\Gamma. \end{aligned} \quad (67)$$

Since  $ds_s > 0$ , from (67) it follows that  $\delta Q > 0$  for  $d\Gamma > 0$ , *i.e.* the process of adsorption leads to heat generation. This observation is also consistent with the fact that normally in the process of adsorption the surfactant goes spontaneously ( $\delta W < 0$ ) from the high chemical potential region (bulk) to the lower chemical potential region (interface) – this difference in chemical potentials is released as heat. Altogether, the first law (1) suggests that in order to maintain the internal surface energy  $U_s = \text{const}$  (and temperature  $T = \text{const}$  if the surfactant concentration is dilute so that it can be considered as a 2D ideal gas, *cf.* Section 5.1) while increasing the entropy, heat must be released.

Another source of heat generation is due to viscous dissipation inevitable when Marangoni stresses operate based on (31). Assuming that all this viscous dissipation is converted into heat, let us estimate the temperature increase. If the variation of surface concentration  $\Delta\Gamma$  occurs over the distance  $l$ , the parameter  $\alpha$  defined in Section 4.4 can be estimated as  $\alpha = \Delta\Gamma/l$  and from (40) we find that over the characteristic time of the Marangoni-driven cycle (49) the change in the bulk internal energy:

$$\Delta U = \frac{\mu}{\rho} \left( \frac{\Delta\sigma}{\Delta\Gamma} \frac{\Delta\Gamma}{\mu l} \right)^2 h \Delta t = \frac{\Delta\sigma}{\rho} = c_p \Delta T, \quad (68)$$

so that per unit mass  $\Delta U$  [ $\text{J kg}^{-1}$ ] =  $\Delta\sigma/(\rho h)$ . This result applies to other geometries as well, *e.g.* for a drop  $l \sim h$  would be its diameter. Then, say, for water as a working medium – under constant pressure the increase in internal energy is  $\Delta U = (c_p - \alpha_T p V) \Delta T$ , where in the second term  $\alpha_T$  is the coefficient of thermal expansion (under constant pressure, accordingly). For systems of the sizes we are interested in, this term can be neglected and hence from (68)  $\Delta T = \Delta\sigma/(\rho c_p) = O(10^{-2})$  K, where we used the value of specific heat capacity  $c_p = 4.2$  J (g K) $^{-1}$  under room temperature of 20 °C. Regardless of the nature of the interfacial chemical reaction such a temperature increase is negligible and for most environmental conditions is diffused away to surroundings, which justifies the idea that Marangoni-driven engines are almost isothermal for most practical purposes.

Finally, since the interface has its own entropy, one can define an effective “thermal” interface of (time-dependent) thickness equal to

the thermal diffusion length, which is according to the Fourier law is  $\sim \sqrt{\kappa t}$ , where  $\kappa$  is the thermal diffusion coefficient. If this length is small compared to the extension of the bulk of the fluid, then one can speak of the different bulk  $T_b$  and interfacial  $T_s$  temperatures. It is not unusual to speak of the interfacial properties separate from that of the bulk. For example, when soap film is being stretched, it absorbs heat from surroundings because of the processes happening at the interface, but not in the bulk. One can say that the temperature of the interface is being dropped in the process of stretching, while this is not what is happening in the bulk; of course, the temperature in the bulk of the soap film will also (eventually) drop because of the heat exchange between the interface and the bulk. If the heat is generated or lost (as in the case of stretching soap film which requires heat to be absorbed from surroundings in order to maintain constant temperature or in the case of chemical reaction at the interface), then it takes  $l^2/\kappa$  time to diffuse over the system of extent  $l$ .

#### 5.4 Energy output and efficiency

Using the definition (3) of thermal efficiency  $\eta = W_{\text{out}}/Q_{\text{in}}$  and the first law of thermodynamics (1), where the work consists of the work done by pressure forces and non-expansion (ne) work,  $\delta W = -PdV + \delta W_{\text{ne}}$ , we can focus on a constant pressure process, thus naturally bringing us to the enthalpy  $H$ :

$$dH = \delta Q + \delta W_{\text{ne}}, \quad (69)$$

which for reversible processes, *i.e.* when  $\delta Q = Tds$ , gives  $dH - Tds = -\delta W_{\text{ne}}$ . The left hand-side of this expression is the Gibbs free energy,  $dG = dH - Tds = \mu dN$  under constant temperature processes. Hence,  $\delta W_{\text{ne}} = -dG$ .

Since the heat input is  $\delta Q_{\text{in}} = -dH$ , then

$$\eta = \frac{dG}{dH} = \frac{dH - Tds}{dH}. \quad (70)$$

Note that the enthalpy change for any reaction that releases energy is negative, while the entropy change can be both negative and positive. If  $ds > 0$ , the reaction will absorb additional heat from the surroundings, so that  $\delta Q_{\text{in}} = -dH + Tds$  and therefore

$$\eta = 1 \text{ for } ds > 0 \text{ and } \eta < 1 \text{ for } ds < 0. \quad (71)$$

Thus, the ideal efficiency  $\eta = 1$  is theoretically achievable for such systems. Since  $G = \mu_i N_i$ , the work is done either by the change of the chemical potential  $\mu_i$  or the number of particles  $N_i$  or both. Hence, at least theoretically, the efficiency can be close to 1.

It is also useful to look at the energy output from the point of view of a chemical potential, which is the basic measure of the chemical energy in the system. If we use the equation  $\mu = \mu^{(0)} + RT \ln C$  for the chemical potential of a non-ionic surfactant and the equilibrium Henry isotherm  $\Gamma = K_H C$ , then the work density relationship (36) under the assumption that  $\sigma' = \sigma_\Gamma = -K = \text{const}$  gives the following density of stored energy

$$\frac{\delta W}{\delta A} = K K_H \frac{\mu - \mu^{(0)}}{RT} e^{-\frac{\mu - \mu^{(0)}}{RT}}, \quad (72)$$

which is positive and thus consistent with (36); here we used the fact that  $\Gamma|_{\mu=\mu^{(0)}} = K_H$ . The expression (72), which is positive

in view of  $\sigma' < 0$ , suggests that the higher the deviation of the chemical potential from its reference state  $\mu^{(0)}$  due to (local) compression of the interface (so that the surfactant concentration increases), the higher the work density.

It is also interesting to relate this observation to the monolayer compressibility<sup>85</sup> defined in terms of the surface chemical potential  $\mu$  and the molecular area  $a$ :

$$\beta_s \equiv -\frac{1}{a} \left( \frac{\partial a}{\partial \pi} \right)_T = -\frac{\partial a}{\partial \mu} \Big|_T, \quad (73)$$

where the slope  $\partial a / \partial \mu$  is clearly negative and thus the compressibility coefficient is positive: the more compactly situated the molecules (smaller  $a$ ) are the higher is their chemical potential  $\mu$ . From (73) it follows that the lower the compressibility, *i.e.* less steep the graph of  $a(\mu)$ , the smaller the change in  $a$  for the same increment in chemical potential  $\Delta\mu$  or, conversely, for the same  $\Delta a$  there will be higher  $\Delta\mu$  for lower  $\beta_s$ . Thus, in order to achieve higher chemical potential  $\mu$  for the same decrease in the molecular area  $\Delta a < 0$ , it is better to have a lower monolayer compressibility coefficient  $\beta_s$ .

### 5.5 On the material behavior $\sigma(T, \Gamma)$

In Section 4.3 we encountered the second derivative  $\sigma_{\Gamma\Gamma}$  and in Sections 5.2 and 5.3 we inevitably arrived at the mixed derivative  $\sigma_{T\Gamma}$ , the sign of which affects the thermodynamic response of a liquid interface. Hence, it is natural to appeal to the stability of matter *via* deducing appropriate thermodynamic inequalities.<sup>84</sup> Since we are interested in variations of  $\Gamma$  (or, equivalently, the surfactant amount  $N_s$ ) and  $T$  under constant volume  $V$  and area  $A$ , *i.e.* the process is both isochoric and isochoric, it is natural to consider the Helmholtz free energy  $F = F_b + F_s$  with the appropriate surface and bulk parts:

$$F_b = U_b - TS_b = -pV, \quad (74a)$$

$$F_s = U_s - TS_s = \mu N_s + \sigma A, \quad (74b)$$

having the corresponding differentials

$$dF_b = -S_b dT - p dV, \quad (75a)$$

$$dF_s = \mu dN_s + \sigma dA - S_s dT. \quad (75b)$$

Calculating the variation of the total free energy  $F$ :

$$\begin{aligned} \delta F &= \frac{\partial F}{\partial T} \delta T + \frac{\partial F}{\partial N_s} \delta N_s \\ &+ \frac{1}{2} \left( \frac{\partial^2 F}{\partial T^2} \delta T^2 + 2 \frac{\partial^2 F}{\partial T \partial N_s} \delta T \delta N_s + \frac{\partial^2 F}{\partial N_s^2} \delta N_s^2 \right) + \dots, \end{aligned} \quad (76)$$

and taking into account that

$$\frac{\partial F}{\partial T} = -S = -S_b - S_s, \quad \frac{\partial F}{\partial N_s} = \mu, \quad (77)$$

we find that a small deviation from an equilibrium, at which  $F$  is minimized, obeys:

$$\frac{\partial^2 F}{\partial T^2} \delta T^2 + 2 \frac{\partial^2 F}{\partial T \partial N_s} \delta T \delta N_s + \frac{\partial^2 F}{\partial N_s^2} \delta N_s^2 > 0. \quad (78)$$

In the case when  $\mu = \text{const}$  we conclude that

$$\frac{\partial^2 \sigma}{\partial T^2} \delta T^2 + 2 \frac{\partial^2 \sigma}{\partial T \partial \Gamma} \delta T \delta \Gamma + \frac{\partial^2 \sigma}{\partial \Gamma^2} \delta \Gamma^2 > 0, \quad (79)$$

whose positive definiteness in turn implies

$$\sigma_{TT} \sigma_{\Gamma\Gamma} - (\sigma_{T\Gamma})^2 > 0, \quad (80)$$

*i.e.*  $\sigma_{TT}$  and  $\sigma_{\Gamma\Gamma}$  must have the same sign, while  $\sigma_{T\Gamma}$  can assume any sign.

If, however, the chemical potential  $\mu$  is not constant, but a function of both temperature  $T$  and concentration  $\Gamma$ , instead of the condition (80) we get

$$(\sigma_{TT} + \Gamma \mu_{TT})(\sigma_{\Gamma\Gamma} + 2\mu_{\Gamma} + \Gamma \mu_{\Gamma\Gamma}) - (\sigma_{T\Gamma} + \Gamma \mu_{T\Gamma} + \mu_T)^2 > 0, \quad (81)$$

If  $\mu$  is a linear function of the temperature  $T$ , then, as one of the two options, there must be  $\sigma_{TT} > 0$  and  $\sigma_{\Gamma\Gamma} > -2\mu_{\Gamma} - \Gamma \mu_{\Gamma\Gamma}$ , where it is known that  $\mu_{\Gamma} < 0$ . Hence, there is a possibility for both  $\sigma_{TT}$  and  $\sigma_{\Gamma\Gamma}$  to have different signs.

## 6 Conclusions and applications

In the presented work we started by drawing a parallel between homogeneous heat engines and chemical ones with the corresponding efficiency computed for both Carnot-type (10) and endoreversible cycles. However, as was demonstrated next, standard thermodynamic cycles are not able to explain the operation of systems, in which energy is stored on inhomogeneities. Proper modification of the thermodynamic cycle approach for distributed systems was offered, which allowed us to understand the role of singularities in thermodynamic terms as well, and to estimate the period of Marangoni-driven cycles (49). The corresponding energy storage was computed both in 3D for pressure gradient-driven systems (26) and in 2D for interfacial surface tension gradient-driven systems (35). A connection to Shannon entropy was established. A thin film example was used to highlight the mechanism of energy storage and dissipation, for both insoluble and soluble surfactants. In the latter case the effect of kinetics was explored with the finding that part of energy (44) can be stored in the bulk as well.

Next, a detailed thermodynamic study of surface tension gradient-driven systems was performed. In particular, intrinsic irreversibility of interfacial processes in systems with surface tension dependent on both temperature and surfactant concentration  $\sigma(T, \Gamma)$  was analyzed. Naturally, the expression for surface entropy (64) was found in the general case of  $\sigma(T, \Gamma)$ , which corrected the classical Kelvin's formula. Isothermality of Marangoni-driven engines has been evaluated quantitatively with the contributing factors due to dissipation and adsorption. Since second derivatives of  $\sigma(T, \Gamma)$  naturally appear in all these analyses, the material behavior  $\sigma(T, \Gamma)$  was explored from the point of view of thermodynamic inequalities (80) and (81). The discussion is concluded with estimates of the energy efficiency (71) and density (72) of such engines.

Just to provide a general context for the presented study, it is worthwhile to look at the causes and consequences. Though forces (such as temperature gradient) and flows (such as the heat flow) are coupled, the possible coupling is restricted by a general symmetry principle. This principle, attributed to Curie and Prigogine,<sup>86</sup> states that macroscopic causes always have fewer or equal symmetries than the effects they produce, *i.e.* that vectorial variables cannot be coupled to scalar variables in isotropic systems in the framework of linear coupling. However, such fluxes can be interrelated at the system interfaces (which are not isotropic) by the boundary conditions. Since chemical energy is a function of concentration of reagents, which are scalars, then to transduce chemical energy to motion either isotropy or linearity must be broken. Clearly, non-linearity may come into our problem from the interfacial conditions (31). However, in our case, all processes can be deemed linear as demonstrated with the help of the thin film example in Section 4.4, *i.e.* there is no need for a nonlinear equation of state or nonlinear boundary conditions. Instead, the mere presence of an interface breaks the assumption of isotropy made by Curie and Prigogine.

In conclusion, if one can identify geometries relevant for the useful conversion of chemical energy into mechanical energy, they can be exploited to perform a number of functions such as pumping, propulsion, and mixing currently accomplished with complex machinery and active control. While the key motivating experiments discussed in Section 2 provide fundamental insights into the conversion of chemical-to-mechanical energy, it will be most useful if there is a practical application for the harnessed energy. We propose the following basic prototypes that can utilize the introduced fundamental ideas (chemical waves, tip-streaming, and oscillating lenses) discussed in Section 2.

- Tip-streaming: noting that the external fluid is set into motion due to Marangoni stresses, *cf.* Fig. 6, their entraining effect can be used as a type of “pump”. To be functional, this pump must be connected to a network of channels and tubes for supply and discharge. The application will involve embedding the basic setup in Fig. 6 with a monolithic fluidic structure in Fig. 17a: the capillary is replaced by a short channel segment and the cuvette of liquid by a T-shaped set of channels.

- Chemical waves: the rotation of chemical waves in the annular container, sketched in Fig. 5, lends itself to the transfer of rotational motion through a paddle-like device, *cf.* Fig. 17b. The application would be to power a generator or a mechanical drive train, for example.

- Oscillating liquid lens: no use for these oscillating liquid lenses has been offered before, but their motion may be utilized to transport the supporting liquid, *e.g.* water in the case of oil lenses. The “beating” motion of oil lens is reminiscent of a flexible membrane operating as a displacement pump. The coupling of oscillating lenses with appropriate channel geometry, similar to the asymmetrical structure of a valveless nozzle-diffuser pump,<sup>87</sup> may result in pumping of the liquid supporting the lens, *cf.* Fig. 17c. Namely, same as the deflection of a membrane or diaphragm is used to pull and push fluid into and out of a reservoir in the nozzle-diffuser pump, the oscillating lens with its spread and recoil action can be the basis for an oscillating lens “pump”. The nozzle and diffuser act as flow rectifying elements, essentially passive valves, due

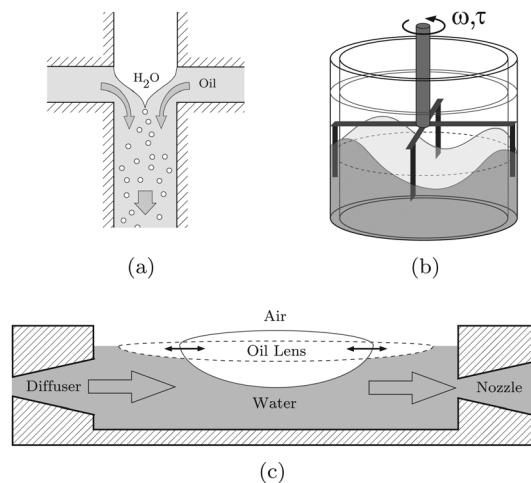


Fig. 17 Examples of applications of the Marangoni phenomena: (a) fluidic network, (b) paddle motor, (c) pump.

to the variable resistance to flow that these parts possess depending upon the direction of fluid motion. A major advantage of a valveless nozzle-diffuser pump is the minimized number of moving mechanical parts which results in less wear, fatigue, and chances of blocking. Such a design would eliminate the fabrication and assembly of membranes and other mechanical components typically found in such devices. Fig. 17c shows a basic schematic of the pump, where the open arrows indicate the net motion of the fluid.

Therefore, potential applications of Marangoni-driven phenomena may range from fluidic operations in various devices, *e.g.* pumping and mixing, to engines. Even though the size of such devices is on the order of centimeters and less, if they find many applications or can be integrated in multiple device platforms the cumulative energy savings may be substantial. Moreover, in certain situations devices powered by chemical Marangoni effects may represent the only alternative due to inability to use other energy sources, *e.g.* when temperature gradients or electric fields may be destructive to the local environment.

## Appendix

### A On Kelvin's derivation

Same as assumed by Kelvin<sup>81,83</sup> we will consider a process in the cycle, shown in Fig. 18, during which the bulk does not perform any work. To determine the work done by the interface during this cycle let us consider two paths on which the interface performs work:

$$\begin{aligned}
 & 1 - 2:\sigma(T + dT, \Gamma + d\Gamma)(A + dA) - \sigma(T + dT, \Gamma)A \\
 & = \left[ \sigma(T, \Gamma) + \frac{\partial\sigma}{\partial T} dT + \frac{\partial^2\sigma}{\partial T^2} \frac{(dT)^2}{2} \right] dA \\
 & + \left[ \frac{\partial\sigma}{\partial \Gamma} d\Gamma + \frac{\partial^2\sigma}{\partial \Gamma^2} \frac{(d\Gamma)^2}{2} + \frac{\partial^2\sigma}{\partial T\partial\Gamma} d\Gamma dT \right] A \\
 & + \left[ \frac{\partial\sigma}{\partial \Gamma} d\Gamma + \frac{\partial^2\sigma}{\partial \Gamma^2} \frac{(d\Gamma)^2}{2} + \frac{\partial^2\sigma}{\partial T\partial\Gamma} d\Gamma dT \right] dA,
 \end{aligned} \tag{82}$$

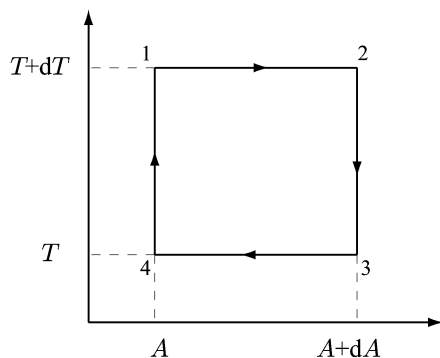


Fig. 18 Carnot-type cycle in Kelvin's analysis<sup>81,83</sup> revisited for the case when the surface tension is a function of two variables, temperature  $T$  and surface concentration  $\Gamma$ .

$$\begin{aligned} 3 - 4: & \sigma(T, \Gamma)A - \sigma(T, \Gamma + d\Gamma)(A + dA) \\ & = -\sigma(T, \Gamma)dA - \left[ \frac{\partial \sigma}{\partial \Gamma} d\Gamma + \frac{\partial^2 \sigma (d\Gamma)^2}{2} \right] A \\ & \quad - \left[ \frac{\partial \sigma}{\partial \Gamma} d\Gamma + \frac{\partial^2 \sigma (d\Gamma)^2}{2} \right] dA + \text{h.o.t.}, \end{aligned} \quad (83)$$

which altogether yield

$$\delta W = \left[ \frac{\partial \sigma}{\partial T} - \Gamma \frac{\partial^2 \sigma}{\partial T \partial \Gamma} \right] dT dA; \quad (84)$$

here we took into account the (insoluble) surfactant amount conservation,  $A\Gamma = \text{const}$ :

$$\frac{d\Gamma}{\Gamma} = -\frac{dA}{A} + \left( \frac{dA}{A} \right)^2 + \dots \quad (85)$$

The interface absorbs the amount of heat  $\delta Q'$  at the temperature  $T' = T + dT$  and gives up  $\delta Q$  at the temperature  $T$ . On the paths 2–3 and 4–1 the interface does not perform any work,  $\delta W = 0$ , since the area stays constant. Conservation of energy requires that  $\delta W = \delta Q' - \delta Q$  or, since for this cyclic transformation the amount of entropy received on the path 2–3 and rejected on the path 4–1 must be equal  $\delta Q/T = \delta Q'/T'$ ,

$$\delta W = \frac{dT}{T} \delta Q. \quad (86)$$

Setting  $\delta Q/T = dS_s$ , where  $S_s$  is the surface entropy, we have from (84) and (86):

$$dS_s = - \left[ \frac{\partial \sigma}{\partial T} - \Gamma \frac{\partial^2 \sigma}{\partial T \partial \Gamma} \right] dA, \quad (87)$$

from which the surface entropy density per unit area follows

$$s_s = \frac{dS_s}{dA} = -\frac{\partial \sigma}{\partial T} + \Gamma \frac{\partial^2 \sigma}{\partial T \partial \Gamma}, \quad (88)$$

clearly being different from (64) in the last term. The reasons for this discrepancy are that (a) the work done by the interface should also involve chemical potential changes and (b) the heat supplied on path 2–3 to drop the temperature need not be equal to that on path 4–1. The above derivation worked for

Kelvin only because he neglected the adsorbed surfactant (and hence chemical potential), without which, ironically, a soap film cannot exist.

## Acknowledgements

This work was partially supported by the National Science Foundation (NSF) CAREER award under Grant No. 1054267 and the Natural Sciences and Engineering Research Council of Canada (NSERC) under Grant No. 6186. The author would also like to thank Andrei Zelnikov for many stimulating discussions, Hans Mayer for the help with figures, and Quinton Farr for reading over the manuscript.

## References

- 1 J. H. Miller, V. Vajrala, H. L. Infante, J. R. Claycomb, A. Palanisami, J. Fang and G. T. Mercier, Physical mechanisms of biological molecular motors, *Physica B*, 2009, **404**, 503–506.
- 2 A. R. Bausch and K. Kroy, A bottom-up approach to cell mechanics, *Nat. Phys.*, 2006, **2**, 231–238.
- 3 F. Cottone, H. Vocca and L. Gammaitoni, Nonlinear energy harvesting, *Phys. Rev. Lett.*, 2009, **102**, 080601.
- 4 U. Seifert, Conformal transformations of vesicle shapes, *J. Phys. A: Math. Gen.*, 1991, **24**, L573–L578.
- 5 E. Sackmann, H.-P. Duwe and H. Engelhardt, Membrane bending elasticity and its role for shape fluctuations and shape transformations of cells and vesicles, *Faraday Discuss. Chem. Soc.*, 1986, **81**, 281–290.
- 6 H. J. Deuling and W. Helfrich, Red blood cell shapes as explained on the basis of curvature elasticity, *Biophys. J.*, 1976, **16**, 861–868.
- 7 S. J. Singer and G. L. Nicolson, The fluid mosaic model of the structure of cell membranes, *Science*, 1972, **175**, 720–731.
- 8 R. A. Capaldi, Dynamic model of cell-membranes, *Sci. Am.*, 1974, **230**, 27–33.
- 9 G. L. Nicolson, The interactions of lectins with animal cell surfaces, *Int. Rev. Cytol.*, 1974, **39**, 89–120.
- 10 L. Wolpert and D. Gincell, *Aspects of cell motility, Symposium of the Society of Experimental Biology XXII*, 1968, pp. 169–198.
- 11 H. I. Virgin, *Aspects of cell motility, Symposium of the Society of Experimental Biology XXII*, 1968, p. 329.
- 12 B. Chance, E. K. Pye and B. Hess, *Biochemical oscillations*, Academic Press, New York, 1971.
- 13 V. B. Fainerman, D. Mobius and R. Miller, *Surfactants: chemistry, interfacial properties, applications*, Elsevier, 2001.
- 14 M. J. Rosen, *Surfactants and interfacial phenomena*, John Wiley & Sons, 1978.
- 15 K. J. Mysels, Surface tension of solutions of pure sodium dodecyl sulfate, *Langmuir*, 1986, **2**, 423–428.
- 16 C. I. Chiwetelu, V. Hornof and G. H. Neale, Interaction of aqueous caustic with acidic oils, *J. Can. Pet. Technol.*, 1989, **28**, 71–78.
- 17 R. Miller, P. Joos and V. Fainermann, Dynamic surface and interfacial tensions of surfactant and polymer solutions, *Adv. Colloid Interface Sci.*, 1994, **49**, 249–302.

- 18 C.-H. Chang and E. Franses, Adsorption dynamics of surfactants at the air/water interface: a critical review of mathematical models, data, and mechanisms, *Colloids Surf.*, 1995, **100**, 1–45.
- 19 S. S. Dukhin, G. Kretzschmar and R. Miller, *Dynamics of adsorption at liquid interfaces*, Elsevier, Amsterdam, 1995.
- 20 A. I. Rusanov and V. A. Prokhorov, *Interfacial tensiometry*, Elsevier, Amsterdam, 1996.
- 21 J. A. Clements, J. Nellenbogen and H. J. Trahan, Pulmonary surfactant and evolution of the lungs, *Science*, 1970, **169**, 603–604.
- 22 M. Grunze, Driven liquids, *Science*, 1999, **283**, 41–42.
- 23 H. Haidara, L. Vonna and J. Schultz, Surfactant induced Marangoni motion of a droplet into an external liquid medium, *J. Chem. Phys.*, 1997, **107**, 630–637.
- 24 F. Blanchette, Simulation of mixing within drops due to surface tension variations, *Phys. Rev. Lett.*, 2010, **105**, 074501.
- 25 S. Berg, Marangoni-driven spreading along liquid-liquid interfaces, *Phys. Fluids*, 2009, **21**, 032105.
- 26 O. O. Ramdane and D. Quéré, Thickening factor in Marangoni coating, *Langmuir*, 1997, **13**, 2911–2916.
- 27 A. Q. Shen, B. Gleason, G. H. McKinley and H. A. Stone, Fiber coating with surfactant solutions, *Phys. Fluids*, 2002, **14**, 4055–4068.
- 28 H. C. Mayer and R. Krechetnikov, Landau-Levich flow visualization: revealing the flow topology responsible for the film thickening phenomena, *Phys. Fluids*, 2012, **24**, 052103.
- 29 A. S. Basu and Y. B. Gianchandani, Virtual microfluidic traps, filters, channels, and pumps using Marangoni flows, *J. Micromech. Microeng.*, 2008, **18**, 115031.
- 30 D. E. Bennett, B. S. Gallardo and N. L. Abbott, Dispensing surfactants from electrodes: Marangoni phenomenon at the surface of aqueous solutions of (11-Ferrocenylundecyl)trimethylammonium bromide, *J. Am. Chem. Soc.*, 1996, **118**, 6499–6505.
- 31 G. Bai, D. Graham and N. L. Abbott, Role of desorption kinetics in determining Marangoni flows generated by using electrochemical methods and redox-active surfactants, *Langmuir*, 2005, **21**, 2235–2241.
- 32 C. A. Lopez, C.-C. Lee and A. H. Hirs, Electrochemically activated adaptive liquid lens, *Appl. Phys. Lett.*, 2005, **87**, 134102.
- 33 T. S. Sørensen, M. Hennenberg, A. Steinchen and A. Sanfeld, Chemical and hydrodynamical analysis of stability of a spherical interface, *J. Colloid Interface Sci.*, 1976, **56**, 191–205.
- 34 C. V. Sternling and L. E. Scriven, Interfacial turbulence: hydrodynamic stability and the Marangoni effect, *AIChE J.*, 1959, **5**, 514–523.
- 35 J. W. M. Bush and D. L. Hu, Walking on water: biolocomotion at the interface, *Annu. Rev. Fluid Mech.*, 2006, **38**, 339–369.
- 36 G. L. van der Mensbrugge, Sur la tension superficielle des liquides considérée au point de vue de certains mouvements observés à leur surface, *Mém. couronnés l'Acad. Roy. Sci. Belg.*, 1869, **34**, 1–67.
- 37 L. Rayleigh, Measurements of the amount of oil necessary in order to check the motions of camphor upon water, *Proc. R. Soc. London*, 1890, **47**, 364–367.
- 38 F. H. Garner, C. W. Nutt and M. F. Mohtadi, Pulsation and mass transfer of pendent liquid droplets, *Nature*, 1955, **175**, 603–605.
- 39 D. A. Haydon, Oscillating droplets and spontaneous emulsification, *Nature*, 1955, **176**, 839–840.
- 40 J. B. Lewis, Liquid-liquid extraction. The extraction of uranyl nitrate in a wetted wall column, *Trans. Inst. Chem. Eng.*, 1953, **31**, 323–325.
- 41 K. Sigwart and H. Nasselstein, The mechanism of material transfer through the boundaries of two liquid phases, *Z. Ver. Dtsch. Ing.*, 1956, **98**, 453–461.
- 42 M. Dupeyrat and E. Nakache, Direct conversion of chemical energy into mechanical energy at an oil water interface, *Bioelectrochem. Bioenerg.*, 1978, **5**, 134–141.
- 43 H. Kitahata and K. Yoshikawa, Chemo-mechanical energy transduction through interfacial instability, *Phys. D*, 2005, **205**, 283–291.
- 44 N. Magome and K. Yoshikawa, Nonlinear oscillations and Ameba-like motion in an oil/water system, *J. Phys. Chem.*, 1996, **100**, 19102–19105.
- 45 S. Nakata, Y. Hayashima and T. Ishii, Self-motion of a camphoric acid boat as a function of pH of aqueous solutions, *Colloids Surf., A*, 2001, **182**, 231–238.
- 46 S. Slavtchev, M. Hennenberg, J.-C. Legros and G. Lebon, Stationary solutal Marangoni instability in a two-layer system, *J. Colloid Interface Sci.*, 1998, **203**, 354–368.
- 47 H. Kitahata, R. Aihara, N. Magome and K. Yoshikawa, Convective and periodic motion driven by a chemical wave, *J. Chem. Phys.*, 2002, **116**, 5666–5672.
- 48 K. Nagai, Y. Sumino, H. Kitahata and K. Yoshikawa, Mode selection in the spontaneous motion of an alcohol droplet, *Phys. Rev. E: Stat., Nonlinear, Soft Matter Phys.*, 2005, **71**, 065301.
- 49 N. M. Kovalchuk and D. Vollhardt, Marangoni instability and spontaneous non-linear oscillations produced at liquid interfaces by surfactant transfer, *Adv. Colloid Interface Sci.*, 2006, **120**, 1–31.
- 50 N. M. Kovalchuk and D. Vollhardt, Oscillation of interfacial tension produced by transfer of nonionic surfactant through the liquid/liquid interface, *J. Phys. Chem. C*, 2008, **112**, 9016–9022.
- 51 K. Eckert, M. Acker, R. Tadmouri and V. Pimienta, Chemo-Marangoni convection driven by an interfacial reaction: Pattern formation and kinetics, *Chaos*, 2012, **22**, 037112.
- 52 V. Pimienta, M. Brost, N. Kovalchuk, S. Bresch and O. Steinbock, Complex shapes and dynamics of dissolving drops of Dichloromethane, *Angew. Chem., Int. Ed.*, 2011, **50**, 10728–10731.
- 53 V. Pimienta and C. Antoine, Self-propulsion on liquid surfaces, *Curr. Opin. Colloid Interface Sci.*, 2014, **19**, 290–299.
- 54 P. G. de Gennes, The dynamics of reactive wetting on solid surfaces, *Physica A*, 1998, **249**, 196–205.
- 55 F. D. dos Santos and T. Ondaruhu, Free-running droplets, *Phys. Rev. Lett.*, 1995, **75**, 2972–2975.
- 56 J. Thomson, On certain curious motions observable at the surfaces of wine and other alcoholic liquors, *Philos. Mag.*, 1855, **10**, 330–333.

- 57 J. B. Fournier and A. M. Cazabat, Tears of wine, *Europhys. Lett.*, 1992, **20**, 517–522.
- 58 M. Gugliotti and T. Silverstein, Tears of wine, *J. Chem. Educ.*, 2004, **81**, 67–68.
- 59 F. Sebba and H. V. A. Briscoe, The variation of the solubility of unimolecular films with surface pressure, and its effect on the measurement of true surface pressure, *J. Chem. Soc.*, 1940, 114–118.
- 60 F. Sebba, Macrocluster gas–liquid and biliquid foams and their biological significance, *ACS Symp. Ser.*, 1975, **9**, 18–39.
- 61 R. Stocker and J. W. M. Bush, Spontaneous oscillations of a sessile lens, *J. Fluid Mech.*, 2007, **583**, 465–475.
- 62 E. A. van Nierop, A. Ajdari and H. A. Stone, Reactive spreading and recoil of oil on water, *Phys. Fluids*, 2006, **18**, 038105.
- 63 S. Kai, S. C. Muller, T. Mori and M. Miki, Chemically driven nonlinear waves and oscillations at an oil–water interface, *Phys. D*, 1991, **50**, 412–428.
- 64 A. Shioi, K. Katano and Y. Onodera, Effect of solid walls on spontaneous wave formation at water/oil interfaces, *J. Colloid Interface Sci.*, 2003, **266**, 415–421.
- 65 J. Fernandez and G. M. Homsy, Chemical reaction-driven tip–streaming phenomena in a pendant drop, *Phys. Fluids*, 2004, **16**, 2548–2555.
- 66 R. Krechetnikov and G. M. Homsy, On physical mechanisms in chemical reaction-driven tip-streaming, *Phys. Fluids*, 2004, **16**, 2556–2566.
- 67 H. B. Callen, *Thermodynamics and an introduction to thermostatistics*, John Wiley & Sons, 1985.
- 68 N. H. Fletcher, Adiabatic assumption for wave propagation, *Am. J. Phys.*, 1974, **44**, 487–489.
- 69 W. G. Hoover and B. Moran, Pressure-volume work exercises illustrating the first and second laws, *Am. J. Phys.*, 1979, **47**, 851–856.
- 70 L. D. Landau and E. M. Lifshitz, *Fluid mechanics*, Pergamon Press, 1989.
- 71 C. E. Shannon, A mathematical theory of communication, *Bell Syst. Tech. J.*, 1948, **27**(379–423), 623–656.
- 72 R. Defay and I. Prigogine, *Surface tension and adsorption*, John Wiley and Sons, New York, 1966.
- 73 L. W. Schwartz and R. V. Roy, Some results concerning the potential energy of interfaces with nonuniformly distributed surfactant, *Phys. Fluids*, 2001, **13**, 3089–3092.
- 74 E. I. Butikov, Misconceptions about the energy of waves in a strained string, *Phys. Scr.*, 2012, **86**, 035403.
- 75 R. Krechetnikov, Cusps and cuspidal edges at fluid interfaces: existence and application, *Phys. Rev. E: Stat., Nonlinear, Soft Matter Phys.*, 2015, **91**, 043019.
- 76 J. W. Gibbs, *The scientific papers of J.W. Gibbs*, Dover, New York, 1961, vol. 1.
- 77 C. H. Bennett, Demons, engines and the second law, *Sci. Am.*, 1987, **257**, 108–116.
- 78 C. E. Mungan, Irreversible adiabatic compression of an ideal gas, *Phys. Teach.*, 2003, **41**, 450–453.
- 79 D. R. Olander, Compression of an ideal gas as a classroom example of reversible and irreversible processes, *Int. J. Eng. Educ.*, 2000, **16**, 524–528.
- 80 P. Hiemenz and R. Rajagopalan, *Principles of colloid and surface chemistry*, Marcel Dekker, Inc., New York, 1997.
- 81 W. Thomson, On the thermal effect of drawing out a film of liquid, *Proc. R. Soc. London*, 1858, **9**, 255–256.
- 82 R. Becker, *Theory of heat*, Springer, 1967.
- 83 A. Prosperetti, Boundary conditions at a liquid-vapor interface, *Meccanica*, 1979, **14**, 34–47.
- 84 L. D. Landau and E. M. Lifshitz, *Statistical physics*, Pergamon Press, 1958.
- 85 C. Sanchez and E. Leiva, First principles calculations of monolayer compressibilities, *Electrochim. Acta*, 1998, **44**, 1229–1236.
- 86 J. O. Hirschfelder, C. F. Curtiss and R. B. Bird, *Molecular theory of gases and liquids*, John Wiley, New York, 1964.
- 87 Y. Liu, H. Komatsuzaki, S. Imai and Y. Nishioka, Planar diffuser/nozzle micropumps with extremely thin polyimide diaphragms, *Sens. Actuators, A*, 2011, **169**, 259–265.